The Astrophysical Journal, 740:92 (12pp), 2011 October 20 doi:10.1088/0004-637X/740/2/92

IMPROVED CONSTRAINTS ON TYPE Ia SUPERNOVA HOST GALAXY PROPERTIES USING MULTI-WAVELENGTH PHOTOMETRY AND THEIR CORRELATIONS WITH SUPERNOVA PROPERTIES

Ravi R. Gupta[1], Chris B. D'Andrea[1], Masao Sako[1], Charlie Conroy[2], Mathew Smith[3], Bruce Bassett[4,5,6], Joshua A. Frieman[7,8], Peter M. Garnavich[9], Saurabh W. Jha[10], Richard Kessler[7,11], Hubert Lampeitl[12], John Marriner[8], Robert C. Nichol[12], and Donald P. Schneider[13]

[1] Department of Physics and Astronomy, University of Pennsylvania, Philadelphia, PA 19104, USA; ravgupta@physics.upenn.edu
[2] Harvard-Smithsonian Center for Astrophysics, Cambridge, MA 02138, USA
[3] Astrophysics, Cosmology and Gravity Centre (ACGC), Department of Mathematics and Applied Mathematics, University of Cape Town, Rondebosch 7701, South Africa
[4] South African Astronomical Observatory, Observatory 7935, South Africa
[5] Department of Mathematics and Applied Mathematics, University of Cape Town, Rondebosch 7701, South Africa
[6] African Institute for Mathematical Sciences, Muizenberg, Cape Town, South Africa
[7] Department of Astronomy & Astrophysics, University of Chicago, Chicago, IL 60637, USA
[8] Fermilab, Batavia, IL 60510, USA
[9] Department of Physics, University of Notre Dame, Notre Dame, IN 46556, USA
[10] Department of Physics & Astronomy, Rutgers, the State University of New Jersey, Piscataway, NJ 08854, USA
[11] Kavli Institute for Cosmological Physics, The University of Chicago, Chicago, IL 60637, USA
[12] Institute of Cosmology and Gravitation, University of Portsmouth, Portsmouth, PO1 3FX, UK
[13] Department of Astronomy & Astrophysics, The Pennsylvania State University, University Park, PA 16802, USA
Received 2011 April 21; accepted 2011 July 29; published 2011 October 3

ABSTRACT

We improve estimates of the stellar mass and mass-weighted average age of Type Ia supernova (SN Ia) host galaxies by combining UV and near-IR photometry with optical photometry in our analysis. Using 206 SNe Ia drawn from the full three-year Sloan Digital Sky Survey (SDSS-II) Supernova Survey (median redshift of $z \approx 0.2$) and multi-wavelength host-galaxy photometry from SDSS, the *Galaxy Evolution Explorer*, and the United Kingdom Infrared Telescope Infrared Deep Sky Survey, we present evidence of a correlation (1.9σ confidence level) between the residuals of SNe Ia about the best-fit Hubble relation and the mass-weighted average age of their host galaxies. The trend is such that older galaxies host SNe Ia that are brighter than average after standard light-curve corrections are made. We also confirm, at the 3.0σ level, the trend seen by previous studies that more massive galaxies often host brighter SNe Ia after light-curve correction.

Key words: cosmology: observations – galaxies: photometry – supernovae: general

Online-only material: color figures

1. INTRODUCTION

Observations of Type Ia supernovae (SNe Ia) are a key measurement in determining the standard cosmological model. Their empirical luminosity-distance calibration based on relations between SN Ia peak luminosity and both light-curve width and optical colors (Phillips 1993; Hamuy et al. 1996b; Riess et al. 1996) provides evidence for the accelerated expansion of the universe and the existence of dark energy (Riess et al. 1998; Perlmutter et al. 1999). According to the current theory, the progenitor of an SN Ia is a carbon–oxygen white dwarf that approaches the Chandrasekhar limit, resulting in a thermonuclear explosion (Whelan & Iben 1973; Hillebrandt & Niemeyer 2000). However, the exact mechanism by which the progenitor accumulates this mass remains uncertain. Investigations of the physical properties of SN Ia host galaxies can provide insight into the environment in which these progenitor systems form. Furthermore, although SNe Ia are remarkably standardizable, correcting for light-curve width and color still results in a scatter in peak brightness of ∼0.15 mag (Guy et al. 2007; Jha et al. 2007; Conley et al. 2008). Studying how variations in SN Ia luminosities depend on the environment of the progenitor will help reveal the origin of this scatter.

Over the years, several correlations between SNe Ia and the properties of their progenitors and environments have been discovered. For example, intrinsically brighter SNe Ia tend to occur in galaxies with younger stellar populations while fainter ones often occur in passively evolving galaxies (Hamuy et al. 1995, 2000; Sullivan et al. 2006). Studies have also shown that per unit stellar mass, the rate of occurrence of SNe Ia within a galaxy declines with decreasing star formation rate (SFR; van den Bergh 1990; Mannucci et al. 2005; Sullivan et al. 2006). In addition, properties of the progenitors themselves can directly influence light-curve properties of SNe Ia. Theoretical models generally agree that the metallicity of the white dwarf progenitor affects the amount of radioactive ^{56}Ni produced in the thermonuclear explosion, the decay of which powers the light curve of the SN (Höflich et al. 1998; Timmes et al. 2003). Assuming that global metallicity correlates with progenitor metallicity, Gallagher et al. (2005) presented qualitative evidence suggesting that it is more likely that progenitor age, rather than metallicity, is primarily responsible for the variability in SN Ia peak luminosity. The true source of this variability has yet to be determined definitively.

More recently, Gallagher et al. (2008) found that early-type host galaxy metallicity is correlated with residuals on the SN Hubble diagram around the best-fit cosmology. The galaxy mass–metallicity relationship (Tremonti et al. 2004) has led several authors to investigate whether mass is a proxy for this metallicity trend with Hubble residual (HR). Indeed, the latest studies have shown that more massive galaxies tend to host SNe Ia with residuals that are brighter than average after light-curve

correction (Kelly et al. 2010; Lampeitl et al. 2010; Sullivan et al. 2010). Age is another host property that can be estimated, which might more directly influence SN progenitor systems. Gallagher et al. (2008) plotted HR against luminosity-weighted age using optical spectra from 29 early-type host galaxies but found no significant trend. Neill et al. (2009) used optical and UV photometry to calculate luminosity-weighted ages of 166 nearby host galaxies. They found that for the subsample of 22 low-extinction host galaxies, there was a 2.1σ trend indicating that SNe Ia in older hosts have residuals that are brighter than average. However, when the full sample was used, the trend disappeared.

In this work, we use SN Ia host galaxy photometry spanning the ultraviolet, optical, and near-infrared bands, which allows us to constrain stellar masses and ages of host galaxies by comparing the observed photometry to synthetic photometry generated from stellar population synthesis models. Knowledge of these physical properties of host galaxies can improve our understanding of SN Ia progenitors and the diversity of their light curves.

2. DATA

2.1. Supernova Sample and Light-curve Analysis

Our supernova sample consists of the spectroscopically confirmed SNe Ia discovered in the full three-year sample of the Sloan Digital Sky Survey (SDSS-II) Supernova Survey (Frieman et al. 2008). These SNe lie in the redshift range $0.01 < z < 0.42$ with a median redshift of $z \approx 0.2$ and are located in Stripe 82, a 300 deg^2 equatorial strip of sky scanned repeatedly by SDSS-II for three months a year from 2005 to 2007 using a CCD camera on the SDSS 2.5 m telescope (York et al. 2000; Gunn et al. 1998, 2006). Over the course of the Supernova Survey, ~500 SNe were spectroscopically confirmed to be Type Ia (Sako et al. 2008; Holtzman et al. 2008). Unlike previous studies, we make use of the SDSS SN sample over the entire redshift range for this work.

We use the publicly available Supernova Analysis package `SNANA` (Kessler et al. 2009b) along with the `SNANA` implementation of the light-curve fitter SALT2 (Guy et al. 2007) to determine SN properties for our sample based on the SDSS-II photometry (Holtzman et al. 2008; M. Sako et al. 2011, in preparation). We apply the following selection cuts to our sample, similar to those made in the cosmology analysis by Kessler et al. (2009a):

1. at least one measurement with $T_{\rm rest} < -2$ days, where $T_{\rm rest}$ is the rest-frame time, such that $T_{\rm rest} = 0$ corresponds to peak brightness in rest-frame B band;
2. at least one measurement with $T_{\rm rest} > +10$ days;
3. at least one measurement with signal-to-noise ratio (S/N) > 5 for each of the g, r, and i bands; and
4. $\mathcal{P}_{\rm fit} > 0.001$, where $\mathcal{P}_{\rm fit}$ is the SNe Ia light-curve fit probability based on χ^2 per degree of freedom.

These cuts reduce our sample size to 319 SNe.

2.2. SDSS Host Galaxy Identification

The SDSS contains photometric measurements in five optical passbands, *ugriz* (Fukugita et al. 1996). In order to match our SNe with host galaxies, we search the SDSS deep optical stacked images of Stripe 82 (Abazajian et al. 2009) for galaxies within a 0.″25 radius of the SN position, as was done by Lampeitl et al. (2010) and M. Smith et al. (2011, in preparation). We choose the closest galaxy to be the host and require that the host SDSS model magnitude falls in the range $15.5 < r < 23$ to ensure robust photometry. Of the 319 SNe that pass light-curve quality cuts, 14 (4%) do not have identifiable hosts because they fall outside of the SDSS footprint, were too faint to be detected in the co-added images, or had r-band magnitudes outside our allowed range. For the remaining 305 host galaxies, we visually confirm each match is correct by inspecting images with and without the SN. In almost all cases, the host identification is unambiguous. However, a spectroscopic redshift for both the SN and the host galaxy is the only sure way to guarantee a correct match, and this is the case for 80% of the SNe Ia in the Supernova Survey.

2.3. Host Matching and Galaxy Photometry

Since our 305 host galaxies are SDSS-selected, we have *ugriz* photometry for all hosts. Nearly all magnitudes come from the Stripe 82 co-add catalog, although for a few cases where the host is nearby and extended, deblending by the pipeline on the co-added image required that we use the Data Release 7 (DR7) (Abazajian et al. 2009) catalog magnitudes derived from single frames. We use the SDSS model magnitudes which are best for galaxy colors. In addition to optical photometry, we obtain host photometry in the ultraviolet and near-infrared from the *Galaxy Evolution Explorer* (*GALEX*) GR6 and the UKIRT (United Kingdom Infrared Telescope) Infrared Deep Sky Survey (UKIDSS) Data Release 5, respectively. The *GALEX* telescope images in two passbands, far-UV (FUV) and near-UV (NUV; Martin et al. 2005). The UKIDSS passbands are *YJHK* and the photometric system is described in Hewett et al. (2006). The description of the UKIDSS survey is given in Lawrence et al. (2007). Model magnitudes, as defined by SDSS, are not computed by *GALEX* and UKIDSS. Therefore, we use Petrosian magnitudes (Petrosian 1976) for UKIDSS and Kron-like elliptical aperture magnitudes (Kron 1980) for *GALEX* since Petrosian magnitudes are not available in the *GALEX* catalog. The majority of galaxies in our sample are not large in angular size, and so the difference between these magnitudes should not be significant. We exclude UKIDSS objects which have been deblended because of a known error in the pipeline that results in erroneous Petrosian magnitudes for these objects (Smith et al. 2009).

Photometric data were obtained from online catalogs via SQL (structured query language) queries through the SDSS Catalogue Archive Server (CAS),[14] the *GALEX* Multimission Archive at STScI (MAST) CAS,[15] and the UKIDSS WFCAM Science Archive (WSA).[16] The UV and near-IR data were obtained by cross-matching the SDSS host galaxy coordinates with the *GALEX* and UKIDSS catalogs using a 5″ search radius. Of the 305 SDSS host galaxies, 198 (65%) have *GALEX* matches and 178 (58%) have UKIDSS matches within 5″, while 127 (42%) have matches in both *GALEX* and UKIDSS.

We do not require every galaxy to have photometry in all 11 bands (FUV, NUV, *ugrizYJHK*). The addition of UV data helps to constrain age, metallicity, and recent star formation, while near-IR data probe the older stellar populations that compose a large portion of the mass. For example, adding *GALEX* data to SDSS data has been shown to greatly improve estimates of dust optical depth and SFR (Salim et al. 2005).

[14] http://casjobs.sdss.org/CasJobs/.
[15] http://galex.stsci.edu/casjobs/.
[16] http://surveys.roe.ac.uk/wsa/.

3. METHODS

3.1. SN Distance Modulus and Hubble Residuals

The distance modulus for a particular SN Ia in the SALT2 model is given by

$$\mu_{\rm SN} = m_B - M + \alpha x_1 - \beta c, \quad (1)$$

where x_1 (stretch parameter), c (color), and m_B (apparent B-band magnitude at peak) are obtained from SALT2 for each SN by fitting its light curve; α and β are coefficients which we assume to be constant; and M is the absolute magnitude. The distance modulus along with α and β is determined from the output of SALT2 using the program SALT2mu (Marriner et al. 2011), which is part of the SNANA package. SALT2mu is able to calculate α and β independent of cosmology by minimizing the scatter in the Hubble relation in small redshift bins. Values of α and β in this work are computed from the sample of SDSS SNe Ia that pass the light-curve cuts in Section 2.1 and which are either spectroscopically confirmed or photometrically typed and have host redshifts. We find the best-fit values to be $\alpha = 0.121$ and $\beta = 2.82$, and use these to obtain the distance modulus, $\mu_{\rm SN}$. The Hubble constant (which is degenerate with M) is effectively a constant offset to $\mu_{\rm SN}$ and is an input to SALT2mu; we choose $H_0 = 70$ km s^{-1} Mpc^{-1}.

We define Hubble residuals as HR $\equiv \mu_{\rm SN} - \mu_z$, where $\mu_{\rm SN}$ is the distance modulus obtained from SN light curves via SALT2mu and μ_z is the distance modulus calculated from the redshift of the SN and the best-fit cosmology. The best-fit cosmology here is determined by SALT2 based on the first-year SDSS-II SN sample (Kessler et al. 2009a), i.e., $\Omega_{\rm M} = 0.274$, $\Omega_\Lambda = 0.735$.

An SN with an HR > 0 signifies that it is fainter than expected for the best-fit cosmology even after correcting for light-curve shape. Here it is useful to define "underluminous" to refer to SNe Ia with HR > 0 and "overluminous" to refer to SNe Ia with HR < 0. Errors in HR are derived by adding the errors on $\mu_{\rm SN}$ and μ_z in quadrature, where the errors on μ_z are calculated as $[\mu(z + z_{\rm err}) - \mu(z - z_{\rm err})]/2$.

3.2. Galaxy Model Fitting

Stellar population synthesis (SPS) codes are commonly used to create model templates of galaxies based on stellar evolution calculations with the goal of inferring galaxy properties such as mass, age, metallicity, and star formation. We use the Flexible Stellar Population Synthesis code (FSPS version 2.1) developed by Conroy et al. (2009) and updated by Conroy & Gunn (2010) to generate spectral energy distributions (SEDs) of composite stellar populations (CSPs). FSPS is similar to codes such as Bruzual & Charlot (2003) and PÉGASE.2 (Fioc & Rocca-Volmerange 1997; Le Borgne & Rocca-Volmerange 2002), but has increased flexibility in the initial mass function (IMF), dust model, and stellar evolution assumptions compared to other models (Conroy et al. 2009). For this work, we use the BaSeL3.1 spectral library and the Padova isochrones as were used by Conroy et al. (2009). Since we are interested only in relative masses of our host galaxies and are not comparing masses directly with other work, the choice of IMF is not so important; here we adopt the commonly used Chabrier (2003) IMF. For details on FSPS and a comparison of spectral libraries, isochrones, and SPS codes, see Conroy et al. (2009) and Conroy & Gunn (2010).

Our models are generated on a grid of four FSPS parameters: metallicity, $\log[Z/Z_\odot]$, assumed constant over time for each model; $\tau_{\rm dust}$, dust attenuating old stellar light; $\tau_{\rm SF}$, the e-folding timescale of star formation; and $t_{\rm start}$, the time when star formation begins. The CSPs we use here each have exponentially declining SFRs, often called "tau models" [SFR$(t) \propto \exp(-t/\tau_{\rm SF})$], that we allow to be shifted in time by an amount $t_{\rm start}$. For each CSP, star formation is initiated at a time $t_{\rm start}$ after the Big Bang and the rate of star formation declines exponentially thereafter, as dictated by $\tau_{\rm SF}$. We adopt the two-component dust model of Charlot & Fall (2000), in which the dust attenuation factor is $\exp(-\tau_\lambda(t))$ and $\tau_\lambda(t)$ is the optical depth given by

$$\tau_\lambda(t) = \begin{cases} \tau_{10}(\lambda/5500\,\text{Å})^{-0.7} & t \leqslant 10\ \text{Myr} \\ \tau_{\rm dust}(\lambda/5500\,\text{Å})^{-0.7} & t > 10\ \text{Myr}. \end{cases} \quad (2)$$

We fix $\tau_{10} = 3\tau_{\rm dust}$, where τ_{10} is the optical depth of dust surrounding stars younger than 10 Myr and $\tau_{\rm dust}$ is the optical depth of dust surrounding stars of greater age (Charlot & Fall 2000; Kong et al. 2004; Conroy et al. 2009). Table 1 lists the values of the FSPS parameters used to generate our model grid. The limits on the grid values were chosen in an attempt to encompass reasonable values appropriate for the stellar populations of our host galaxy sample. Our redshifts range from nearby to intermediate, indicating that our hosts are likely not extremely metal-poor. The range on $\tau_{\rm dust}$ is centered on the standard value given in Charlot & Fall (2000). An SFR with a $\tau_{\rm SF}$ value of 0.1 Gyr closely resembles a single burst of star formation while a value of 10 Gyr is essentially a flat, constant SFR. The maximum value of $t_{\rm start}$ was chosen to be 7 Gyr after the Big Bang since it is unlikely that *all* stars in a galaxy would be formed later than this.

Table 1
FSPS Model Grid Parameters

FSPS Parameter	Grid Values
$\log[Z/Z_\odot]$	−0.88, −0.59, −0.39, −0.20, 0, 0.20
$\tau_{\rm dust}$	0, 0.1, 0.3, 0.5, 1.0, 1.5
$\tau_{\rm SF}$ (Gyr)	0.1, 0.5, 1, 2, 3, 4, 6, 8, 10
$t_{\rm start}$ (Gyr)	0, 1, 2, 3, 4, 5, 6, 7

The models produce photometry in FUV, NUV, *ugriz*, and *YJHK* for direct comparison with observed data from *GALEX*, SDSS, and UKIDSS. The spectroscopic redshift of the SN is used to obtain the synthetic apparent magnitudes for each model SED. In calculating derived galaxy properties, we assume the aforementioned Kessler et al. (2009a) cosmology ($\Omega_{\rm M} = 0.274$, $\Omega_\Lambda = 0.735$) along with $H_0 = 70$ km s^{-1} Mpc^{-1}, for consistency. Our results are not strongly affected by our choice of cosmology.

All magnitudes are corrected for Milky Way extinction using the maps of dust IR emission from Schlegel et al. (1998) in conjunction with the extinction curve of Cardelli et al. (1989). The SDSS and UKIDSS magnitudes are then corrected to the AB system (Oke & Gunn 1983), using Kessler et al. (2009a) and Hewett et al. (2006), respectively. We add minimum calibration errors from Blanton et al. (2003) in quadrature to all SDSS magnitude errors (0.05, 0.02, 0.02, 0.02, and 0.03 mag for *ugriz*, respectively) to account for systematic effects. For *GALEX* and UKIDSS, we add a minimum calibration error of 0.02 mag in quadrature with the photometric error for each band as well. All magnitudes and errors are converted to flux. A least-squares fit is then performed in flux between the data and each of the model SED fluxes, taking into account the photometric errors.

Analogous to the χ^2 cuts performed on the SNe sample, we remove any galaxies for which the probability of the data being

drawn from the best-fit model is <0.001. This criterion removes one-third of our hosts from our sample and brings the final SN-host sample size to 206. This is the sample we will examine for this study.

3.3. Derived Galaxy Properties

From the fit parameters for each SED model, we derive two physical properties of our host galaxies: stellar mass and mass-weighted average age. Stellar mass (mass currently in stars) is calculated by multiplying the observed, de-reddened luminosity in the r band by the model mass-to-light ratio in the same band. The mass-weighted average age of the galaxy is computed as

$$\langle \mathrm{Age} \rangle = A - \frac{\int_0^A t\Psi(t)dt}{\int_0^A \Psi(t)dt}, \quad (3)$$

where A is the age of the universe at the redshift of the SN minus t_{start} and $\Psi(t)$ is the SFR as a function of time in units of $M_\odot$ yr^{-1}. For each galaxy, we calculate the median mass and age and the corresponding 68% confidence intervals around the median (analogous to a $\pm 1\sigma$ range for a Gaussian distribution). These uncertainties are obtained from the probability density functions (PDFs) constructed for both mass and age from the likelihoods of the models where each model is given a weight $\propto \exp(-\chi^2/2)$. We take this PDF to be a sampled version of the true continuous distribution (which may not be Gaussian). In this way, our mass and age estimates are marginalized over the FSPS parameters such as metallicity and dust. In Table 2, we list the SNe used in our final sample, the host galaxy coordinates, the redshift of the SN, the host galaxy stellar mass and mass-weighted age, the SALT2 color and stretch parameters, and the HR. A complete list of the SNe from years two and three of the SDSS-II Supernova Survey along with photometry and other associated data will be published in M. Sako et al. (2011, in preparation).

4. RESULTS

4.1. Host Galaxy Properties

To determine if adding UV and near-IR photometry to optical data improves constraints on physical properties of our host galaxies, we examine the sample of 71 SDSS galaxies that have matches in both *GALEX* and UKIDSS (after all cuts are made). We find that while adding *GALEX* and UKIDSS data to the SDSS observations does not significantly change our resulting host masses, it does reduce the average uncertainties in the mass estimates (see Figure 1), where the average uncertainty here is the mean of the upper and lower 1σ uncertainties. The uncertainty in mass increases with redshift because the photometric errors increase with redshift, but adding UV and near-IR data reduces these uncertainties in mass overall by 17%. The addition of UV and near-IR data widens the range of the host age distribution while also reducing the average uncertainty in age on the whole by 22% (see Figure 2).

Figure 3 shows a plot of mass-weighted average age versus the stellar mass of our sample of host galaxies. The distribution exhibits the expected trend that, in general, the most massive galaxies are also the oldest. However, there appears to be an absence of low-mass old galaxies. This may be due to several factors, one of which is that for a given mass, older galaxies will be harder to detect by SDSS because they are fainter in the optical due to a dearth of young, bright stars. This absence of small, old galaxies may also be due to the fact that these galaxies likely have a low SFR per unit mass and therefore do not produce many Type Ia events (van den Bergh 1990; Mannucci et al. 2005; Sullivan et al. 2006).

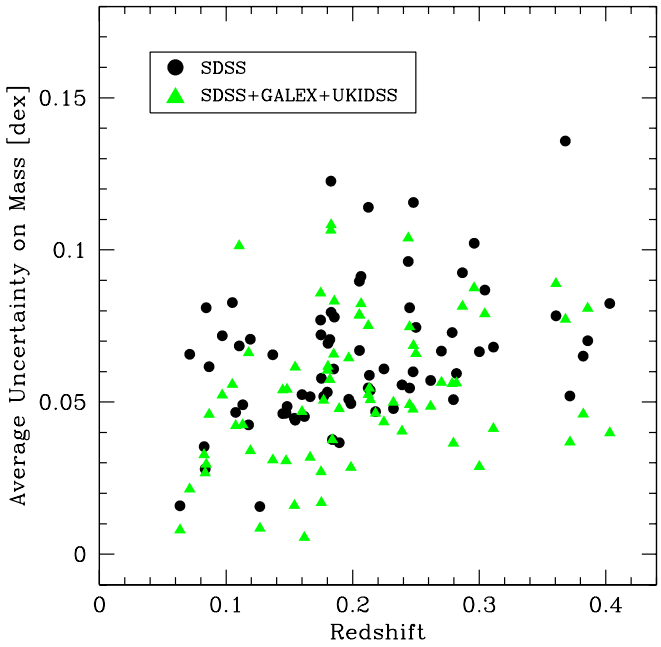

Figure 1. Average mass uncertainty as a function of redshift for the sample of 71 galaxies which have photometry in optical, UV, and near-IR. Black circles indicate results obtained from fits using SDSS data only and triangles indicate results obtained from fits using SDSS, *GALEX*, and UKIDSS data.

(A color version of this figure is available in the online journal.)

4.2. Correlations with SN Fit Parameters

Figure 4 plots the SALT2 SN fit parameters, stretch and color, as a function of host galaxy mass-weighted average age. By definition, higher values of stretch correspond to intrinsically brighter SNe Ia. Our results indicate that intrinsically brighter SNe occur preferentially in younger stellar populations. This is consistent with the known trend that brighter SNe occur in late-type (Hamuy et al. 1996a; Gallagher et al. 2005), star-forming galaxies (Sullivan et al. 2006), and in bluer environments (Hamuy et al. 2000), since these types of galaxies are generally also young. The trend we see of SN color as a function of host age is not as clear; the distribution is essentially flat, although extreme values of color do seem to correlate with age. However, since the SALT2 c parameter encapsulates not only intrinsic SN color but also possible extinction due to dust in the host galaxy, a definitive statement cannot be made about the relation between SN color and host age. Plots of stretch and color versus the host mass are not shown here, though our results strongly resemble those found in Howell et al. (2009), Neill et al. (2009), and Sullivan et al. (2010).

4.3. Linear Trends with Hubble Residuals

Linear regression has a long history in astronomy where there are often measurement errors in both the "dependent" and "independent" variables. There is, however, no consensus on the best method to use when fitting a line. Here, we fit for a linear dependence of HR with age and mass using the package LINMIX (Kelly 2007), as was used to determine the significance of trends with HR by Kelly et al. (2010). LINMIX is a Bayesian approach to linear regression using a Markov chain

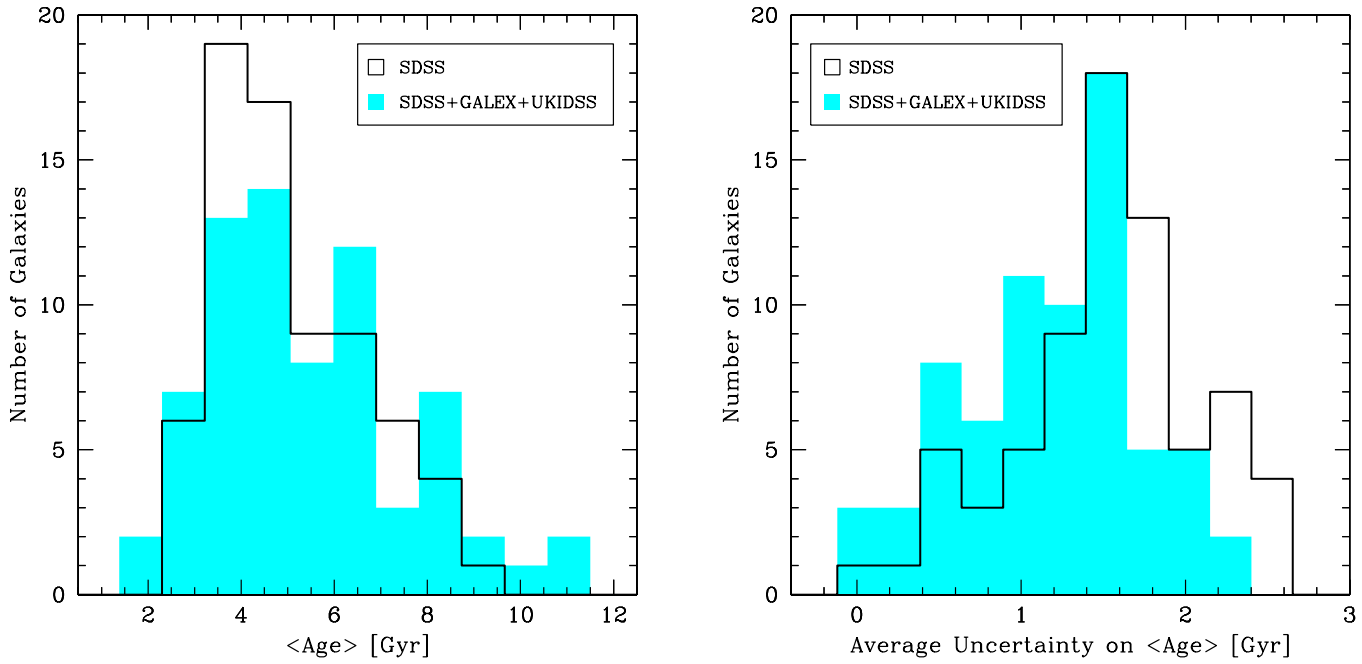

Figure 2. Left: distributions of mass-weighted average age for the sample of 71 galaxies that have photometry in optical, UV, and near-IR, showing the effect of adding *GALEX* and UKIDSS data to SDSS data. Right: distributions of the average uncertainty on the age for the same sample.

(A color version of this figure is available in the online journal.)

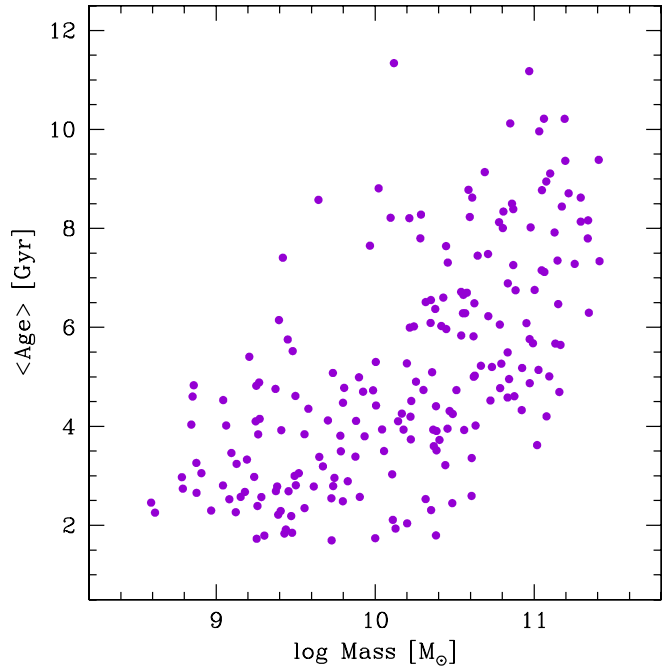

Figure 3. Mass-weighted average age as a function of the stellar mass for our host galaxies. As one would expect, the more massive galaxies tend to be the older galaxies, though the scatter in the relation is large.

(A color version of this figure is available in the online journal.)

Monte Carlo (MCMC) analysis, assuming that the measurement errors are Gaussian. We make the assumption that our errors on the host properties are Gaussian and input into LINMIX the average of the upper and lower 1σ uncertainties as the error in the dependent variable.

When fitting, we do not add the intrinsic uncertainty (0.14 mag for SALT2) in quadrature to the HR errors that is added by others when fitting for trends of host properties with HR (Kelly et al. 2010; Sullivan et al. 2010; Lampeitl et al. 2010). This intrinsic uncertainty arises from the fit to the Hubble diagram and is the amount of scatter that must be added to the distance modulus such that the reduced χ^2 of the best-fit cosmology is close to unity. This is done in an attempt to account for unknown effects on SN Ia luminosity by factors not accounted for in the light-curve correction process, for example, the properties of the host galaxy. The effect of host galaxy properties on SN Ia is precisely the purpose of our study, so including the intrinsic scatter has the effect of weakening the strength of the measured correlations. If we perform the fit including the intrinsic uncertainty, we find that our best-fit slopes and intercepts vary only slightly, but the significances of the non-zero slopes drop by about 0.2σ.

In Figure 5, we plot HR versus the mass-weighted average age of the host galaxy. Figure 6 shows HR versus the stellar mass of the host galaxy. The overplotted lines are the best-fit model as determined from LINMIX. In all our LINMIX analyses, we use 100,000 MCMC realizations. For the HR trend with age, we find the equation of the best-fit line to be

$$\mathrm{HR} = -0.015(\pm 0.008) \times \langle \mathrm{Age} \rangle + 0.071(\pm 0.038). \quad (4)$$

The MCMC realizations in LINMIX are used to generate a sampling of the posterior distribution on the slope. Of the MCMC realizations, 2% have a slope greater than zero. Fitting a Gaussian to the posterior slope distribution yields a mean of -0.015 and a standard deviation of 0.008. Based on this Gaussian fit, the mean slope differs from a slope of zero by 1.9σ. Thus, for the HR–age correlation, we quote the significance of a non-zero slope as 1.9σ. For the HR trend with mass, the best-fit line is

$$\mathrm{HR} = -0.057(\pm 0.019) \times \log M + 0.57(\pm 0.19). \quad (5)$$

Of the MCMC realizations, 0.1% have a slope greater than zero. This corresponds to a 3.0σ significance of a non-zero slope.

Our results indicate that after light-curve correction there appears to be a deficit of underluminous SNe in older, more

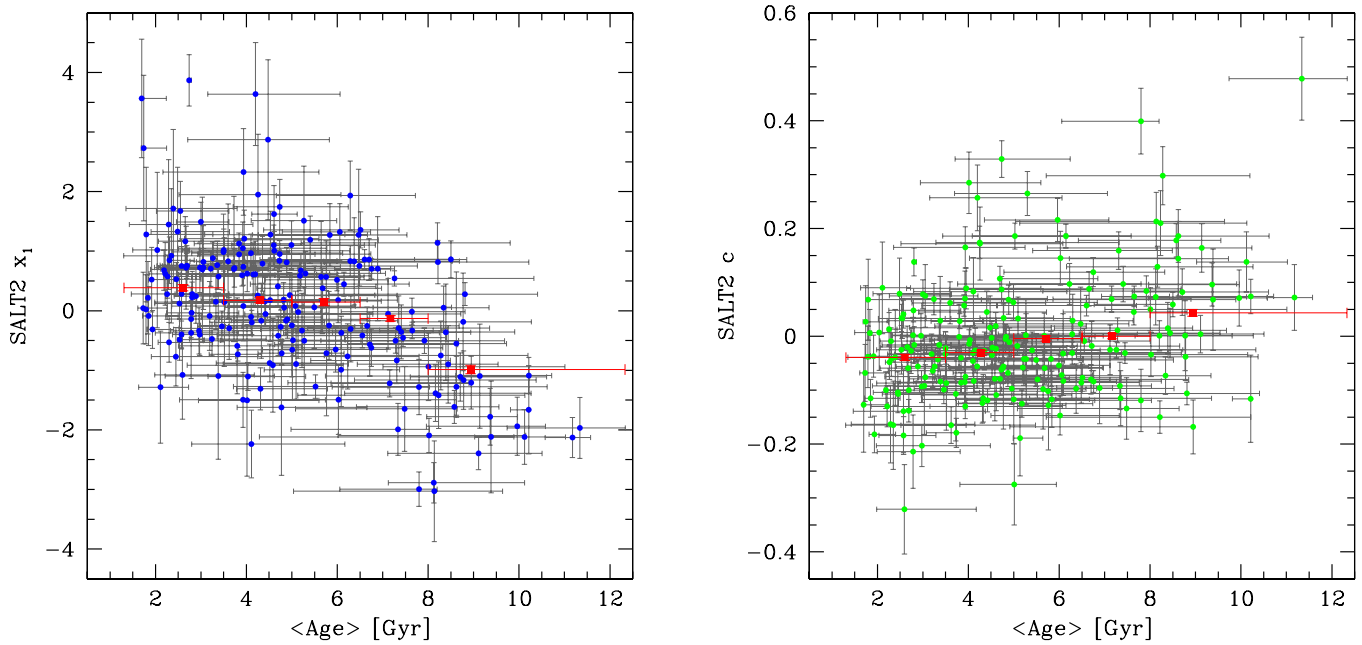

Figure 4. SALT2 stretch (x_1) and color (c) as a function of mass-weighted average age of the host galaxy. The squares are binned averages calculated by taking the mean age and the inverse variance-weighted mean SALT2 parameter in each bin. The error bars show the size of the bin (1.5 Gyr) and the 1σ error on the mean SALT2 parameter.

(A color version of this figure is available in the online journal.)

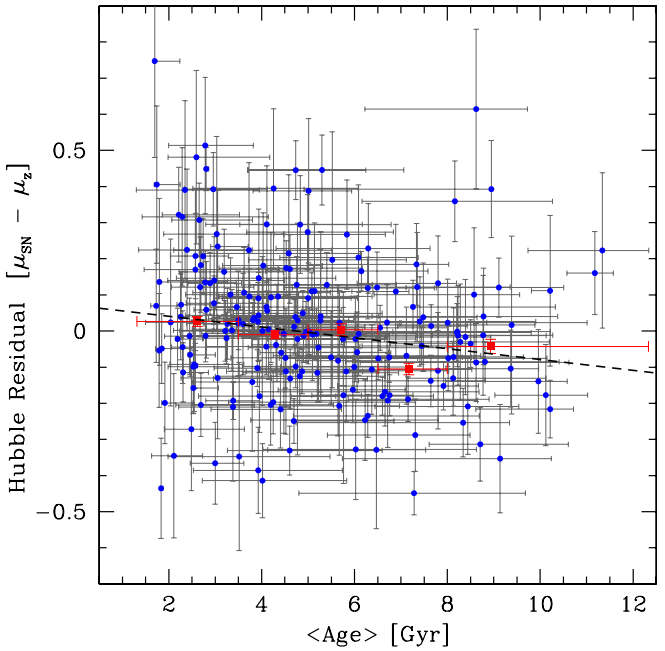

Figure 5. Hubble residual as a function of mass-weighted average age of the host galaxy. The squares are binned averages calculated by taking the mean age and the inverse variance-weighted mean HR in each bin. The error bars show the size of the bin (1.5 Gyr) and the 1σ error on the mean HR. The overplotted line shows the best fit to all the data points as described in Section 4.3 and is given by the equation $\mathrm{HR} = -0.015 \times \langle \mathrm{Age} \rangle + 0.071$. Of the MCMC realizations, 2% have a slope greater than zero, and the significance of the deviation of the best-fit slope from zero is 1.9σ.

(A color version of this figure is available in the online journal.)

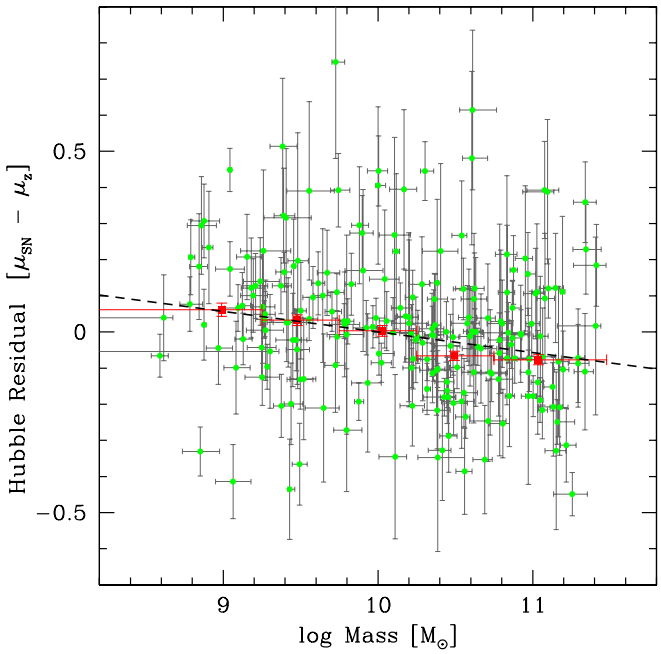

Figure 6. Hubble residual as a function of stellar mass of the host galaxy. The squares are the binned averages as described in Figure 5 and the bin size is 0.5 dex. The overplotted line shows the best fit to all the data points as described in Section 4.3 and is given by the equation $\mathrm{HR} = -0.057 \times \log M + 0.57$. Of the MCMC realizations, 0.1% have a slope greater than zero, and the significance of the deviation of the best-fit slope from zero is 3.0σ.

(A color version of this figure is available in the online journal.)

massive galaxies. To test whether this result is due to incompleteness, we investigated the subsample of 40 SNe Ia for which SDSS is complete ($z \leqslant 0.15$). Up to $z = 0.15$, the SDSS-II SN survey is estimated to be ∼100% efficient for spectroscopic measurement (Kessler et al. 2009a), so any SN Ia that may have occurred should have been detected in this subsample once the host is subtracted from the image. Applying the method used on the full sample to the complete subsample reveals that the trend of HR with mass persists, with a slightly increased significance of 3.4σ. However, the HR trend with age is not statistically significant (1.2σ) for the complete subsample.

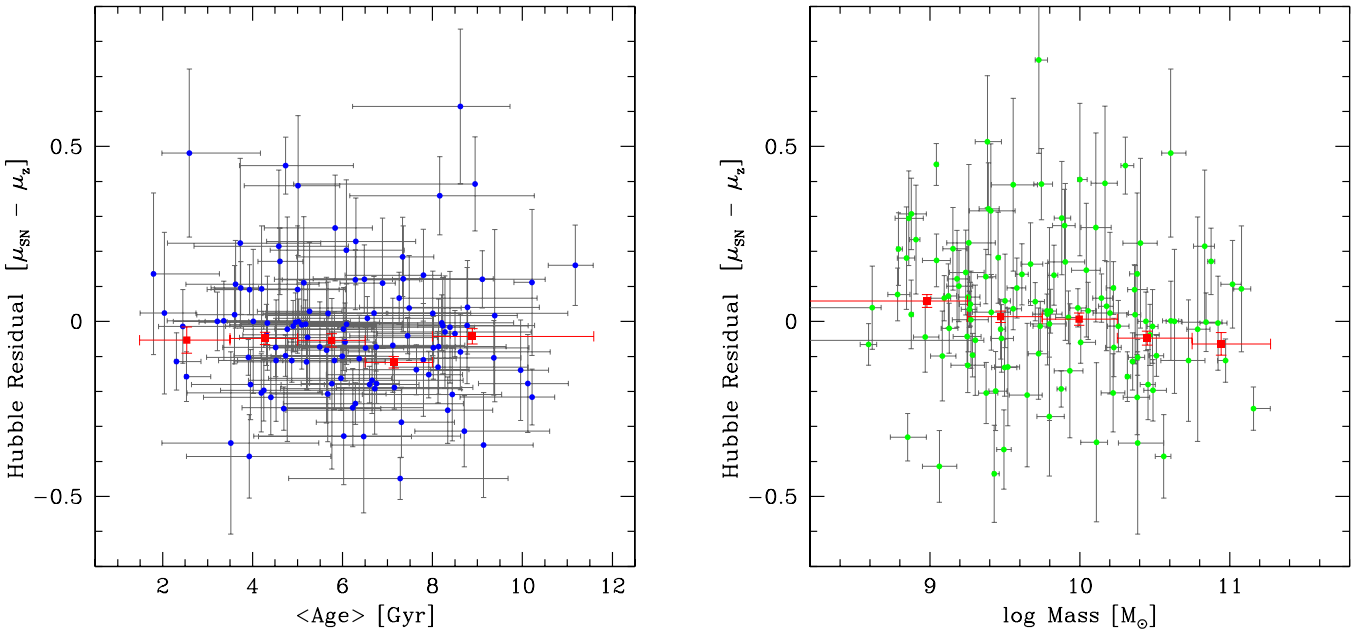

Figure 7. Left: HR vs. host galaxy age for the logMass > 10.2 group. Right: HR vs. host galaxy mass for the ⟨Age⟩ < 5 Gyr group. The squares are the binned averages. (A color version of this figure is available in the online journal.)

4.4. SDSS Co-add versus Single-frame Photometry

We also performed our analysis using SDSS Petrosian magnitudes from the DR7 catalog, which are derived from the single-frame images, in place of the Stripe 82 catalog co-add model magnitudes, which are derived from the stacked images. A comparison of single-frame Petrosian magnitudes with co-add model magnitudes shows the two types of magnitudes agree for the most part, though there is scatter in the difference which increases with magnitude. The *u*-band difference exhibits the largest scatter and a slight bias indicating that the single-frame Petrosian *u*-band magnitudes tend to be brighter.

We find that using single-frame photometry can change the derived galaxy properties and the uncertainties on these properties, thus possibly affecting the significance of trends with HR. The photometric errors on the single-frame magnitudes are roughly 10 times larger than the photometric errors on the co-add magnitudes. As a result, using single-frame magnitudes reduces the χ^2 values of the SED fits and expands the range of SED models that provide reasonable fits, according to our method described in Section 3.3. This then has the effect of potentially shifting the median and increasing the width of the χ^2-weighted PDF for the galaxy properties, which changes our derived values for these properties and increases their uncertainties. The derived galaxy mass is robust and relatively unaffected by the difference between single-frame and co-add photometry, although the uncertainties on the mass are more than twice as large for the single-frame data. The average age is much more sensitive to this difference. Overall, the single-frame Petrosian magnitudes produce younger ages and larger uncertainties on the age, but the scatter in both of these quantities is large. The younger ages may be due in part to the *u*-band magnitude difference, since more flux in bluer bands can be interpreted as light from younger stars. As a test, we inflated the errors on the co-add magnitudes by a factor of 10 and found that the results essentially reproduce those obtained from using the single-frame Petrosian magnitudes, suggesting that the size of the photometric errors plays a substantial role in the discrepancy in derived galaxy properties.

5. DISCUSSION

We confirm with a significance of 3.0σ the result found by Kelly et al. (2010), Sullivan et al. (2010), and Lampeitl et al. (2010) that massive galaxies tend to host overluminous SNe Ia. We also find indication, with a significance of 1.9σ, that even after light-curve correction, overluminous SNe Ia tend to occur in older stellar populations. We note that the Neill et al. (2009) trend of HR with host age was based on luminosity-weighted age, whereas in this work we calculate mass-weighted age, making a direct comparison difficult. However, the direction of the age trend we see agrees with the Neill et al. (2009) trend for their low-extinction hosts. The HR trend with host luminosity-weighted age plotted by Gallagher et al. (2008) is in the opposite direction from the trend we find here, though the significance of their trend is negligible and their methods different. We expect that mass-weighted age is a more unbiased measure of the age of the galaxy because it is not as strongly affected by UV flux from young stars as luminosity-weighted age (see Lee et al. 2007, their Table 1). Furthermore, the mass-weighted age gives more weight to older stellar populations, to which SN Ia progenitors most probably belong, and is therefore more likely to be correlated with SN Ia properties than luminosity-weighted age.

The trends we find of HR with mass and age agree with each other in the sense that galaxy mass and age are correlated, with older galaxies generally being more massive. Based on the mass–age distribution in Figure 3, we split our data into two groups: an ⟨Age⟩ < 5 Gyr group (which encompasses nearly the entire range of masses) and a logMass > 10.2 group (which encompasses nearly the entire range of ages). This was done in an effort to investigate the effect of one of the variables (mass or age) on HR while attempting to "control" for the other. In Figure 7, we plot HR against age for the logMass > 10.2 group and HR against mass for the ⟨Age⟩ < 5 Gyr group. Within these groups we find that the HR correlation with mass is much weaker than in the full sample, and that the HR plot with age is consistent with no correlation. Estimates of host galaxy mass are more robust and have smaller uncertainties than estimates of

Table 2
Properties of SN Ia Sample and Host Galaxies

Designation		Host Coordinates		Redshift[a]	$M-$	M	$M+$	Age$-$	Age	Age+	c	x_1	HR
SN ID	IAU	$\alpha(J2000)$	$\delta(J2000)$			($\log M_\odot$)			(Gyr)				(mag)
1166	...	9.3552761078	0.9739487767	0.38240 ± 0.00050	11.08	11.15	11.22	4.13	6.47	7.53	0.023 ± 0.068	1.274 ± 1.103	−0.3288 ± 0.2179
1253	2005fd	323.7985839844	0.1628694236	0.26200 ± 0.00500	11.27	11.34	11.39	5.89	7.80	8.03	−0.119 ± 0.058	−1.280 ± 0.464	−0.1097 ± 0.1611
1371	2005fh	349.3737487793	0.4296737611	0.11915 ± 0.00012	10.95	11.00	11.02	5.27	6.76	7.26	−0.084 ± 0.020	0.703 ± 0.167	−0.1775 ± 0.0566
1580	2005fb	45.3238296509	−0.6422790885	0.18300 ± 0.00008	10.61	10.73	10.83	3.58	5.20	6.95	−0.058 ± 0.026	0.675 ± 0.271	−0.1156 ± 0.0775
1688	...	321.3578186035	0.3248503506	0.35870 ± 0.00050	10.09	10.20	10.32	1.50	2.04	2.74	0.007 ± 0.070	1.019 ± 1.306	0.0240 ± 0.2309
2017	2005fo	328.9438781738	0.5934827328	0.26160 ± 0.00050	10.48	10.54	10.57	4.26	5.84	6.66	−0.117 ± 0.052	1.272 ± 0.527	0.2671 ± 0.1512
2165	2005fr	17.0916309357	−0.0962756798	0.28800 ± 0.00500	9.33	9.39	9.46	1.86	2.21	3.52	−0.130 ± 0.038	0.620 ± 0.526	0.3219 ± 0.1315
2330	2005fp	6.8073453903	1.1208769083	0.21320 ± 0.00050	9.83	9.88	9.94	2.80	4.11	6.16	0.083 ± 0.063	−2.238 ± 0.569	0.2954 ± 0.1620
2372	2005ft	40.5208168030	−0.5410116911	0.18050 ± 0.00050	10.37	10.45	10.49	6.08	7.64	8.81	0.045 ± 0.024	−0.015 ± 0.225	−0.1379 ± 0.0714
2422	2005fi	1.9945372343	0.6381285191	0.26500 ± 0.00500	9.09	9.15	9.25	2.03	2.57	3.29	−0.184 ± 0.035	0.751 ± 0.326	0.2078 ± 0.1181
2533	2005fs	31.2206439972	−0.3263290226	0.34000 ± 0.00500	9.95	10.04	10.14	2.16	3.94	5.59	−0.075 ± 0.060	2.329 ± 0.727	0.1465 ± 0.1912
2635	2005fw	52.7040061951	−1.2376136780	0.14370 ± 0.00050	9.93	9.99	10.04	3.35	4.73	6.00	−0.062 ± 0.021	0.839 ± 0.183	0.0388 ± 0.0545
2789	2005fx	344.2020263672	0.4005828500	0.29030 ± 0.00050	11.07	11.15	11.20	5.35	7.35	9.35	−0.115 ± 0.051	−0.292 ± 0.543	0.1218 ± 0.1512
2943	2005go	17.7050647736	1.0080429316	0.26540 ± 0.00050	9.00	9.08	9.17	1.99	2.53	3.29	−0.025 ± 0.045	0.121 ± 0.408	−0.0989 ± 0.1285
3080	2005ga	16.9316864014	−1.0394667387	0.17500 ± 0.00050	10.92	10.97	10.97	3.67	4.87	4.87	−0.068 ± 0.025	−0.166 ± 0.244	−0.1118 ± 0.0621
3199	2005gs	333.2925415039	1.0506948233	0.25110 ± 0.00050	8.79	8.88	8.98	2.07	2.66	3.80	−0.020 ± 0.039	1.166 ± 0.414	0.3073 ± 0.1018
3256	2005hn	329.2674865723	−0.2234567255	0.10760 ± 0.00050	9.76	9.81	9.84	4.25	4.78	5.87	0.034 ± 0.034	−0.714 ± 0.198	0.0294 ± 0.0627
3377	2005gr	54.1561660767	1.0789009333	0.24510 ± 0.00050	9.32	9.38	9.45	2.15	2.69	3.84	−0.100 ± 0.034	0.756 ± 0.337	−0.2046 ± 0.0875
3451	2005gf	334.0685424805	0.7077997923	0.25000 ± 0.00050	10.72	10.81	10.85	4.74	8.34	9.34	−0.073 ± 0.035	0.052 ± 0.362	−0.2537 ± 0.0948
3452	2005gg	334.6713256836	0.6394435167	0.23040 ± 0.00050	9.46	9.47	9.50	2.15	2.19	2.73	−0.100 ± 0.034	0.680 ± 0.338	−0.0220 ± 0.0856
3592	2005gb	19.0529479980	0.7905687690	0.08656 ± 0.00019	10.60	10.64	10.69	6.16	7.45	8.40	−0.031 ± 0.019	−0.454 ± 0.146	−0.0411 ± 0.0513
4000	2005gt	31.0166950226	−0.3663079143	0.27860 ± 0.00050	10.89	10.95	11.00	4.39	6.08	7.37	−0.032 ± 0.074	−0.990 ± 0.619	0.2036 ± 0.2011
4046	2005gw	354.4983215332	0.6421458125	0.27700 ± 0.00500	9.15	9.27	9.39	2.51	4.15	6.01	−0.026 ± 0.041	0.609 ± 0.533	0.0048 ± 0.1390
4241	2005gu	12.2376222610	−0.9054884911	0.33200 ± 0.00050	9.19	9.25	9.33	1.61	1.73	2.26	−0.068 ± 0.053	0.044 ± 0.602	0.0697 ± 0.1566
4577	2005gv	38.4758186340	0.2808535695	0.36300 ± 0.00500	10.54	10.73	10.83	3.25	4.52	6.18	−0.035 ± 0.054	0.178 ± 0.691	−0.1117 ± 0.1733
4679	2005gy	21.5282917023	0.6768267751	0.33240 ± 0.00050	9.43	9.52	9.60	2.26	3.05	4.21	0.075 ± 0.058	0.726 ± 0.704	−0.1301 ± 0.1685
5103	2005gx	359.8843383789	0.7369195819	0.16190 ± 0.00050	9.28	9.28	9.30	2.57	2.57	2.62	0.041 ± 0.026	−0.398 ± 0.224	−0.0962 ± 0.0622
5183	2005gq	53.4536514282	0.7093452215	0.38980 ± 0.00050	9.79	9.90	10.03	1.47	2.57	4.37	−0.139 ± 0.077	0.282 ± 0.925	0.1701 ± 0.2238
5391	2005hs	52.3423271179	−1.0952030420	0.30090 ± 0.00050	−99.00	9.30	9.36	1.77	1.79	1.83	−0.038 ± 0.057	0.023 ± 0.581	−0.0537 ± 0.1579
5533	2005hu	328.6699523926	0.4132809639	0.21970 ± 0.00050	9.69	9.74	9.79	2.25	2.79	3.83	0.048 ± 0.021	−0.035 ± 0.336	−0.0135 ± 0.0713
5736	2005jz	22.8627357483	−0.6316036582	0.25300 ± 0.00500	8.89	8.97	9.06	2.06	2.30	3.25	−0.009 ± 0.025	−0.530 ± 0.335	−0.0444 ± 0.1002
5737	2005ib	22.8571491241	−0.6033283472	0.39300 ± 0.00050	9.71	9.80	9.90	1.90	2.49	3.63	0.079 ± 0.066	1.329 ± 1.078	−0.2717 ± 0.1697
5844	2005ic	327.7861633301	−0.8428391814	0.31080 ± 0.00050	9.41	9.48	9.56	1.72	1.85	2.50	−0.115 ± 0.035	−0.087 ± 0.495	−0.0486 ± 0.0965
5944	2005hc	29.2021064758	−0.2125778049	0.04594 ± 0.00017	10.87	10.87	10.92	7.26	7.26	10.33	−0.025 ± 0.015	0.543 ± 0.127	0.0667 ± 0.0739
5957	2005ie	34.7598075867	−0.2725664973	0.27960 ± 0.00050	10.45	10.49	10.52	1.91	2.45	4.25	−0.104 ± 0.038	−0.771 ± 0.489	−0.0143 ± 0.1051
6100	2005ka	333.4833679199	1.0861500502	0.31770 ± 0.00050	9.99	10.00	10.05	1.68	1.74	2.24	0.027 ± 0.067	2.730 ± 1.223	0.4055 ± 0.2179
6196	2005ig	337.6311950684	−0.5023938417	0.28070 ± 0.00050	11.11	11.17	11.23	6.44	8.44	9.54	0.006 ± 0.046	−0.899 ± 0.653	−0.2086 ± 0.1329
6649	2005jd	34.2763099670	0.5356944203	0.31400 ± 0.00500	9.34	9.45	9.54	4.12	5.75	6.50	−0.102 ± 0.042	0.568 ± 0.606	−0.0221 ± 0.1289
6777	2005iy	321.2164306641	0.3856396675	0.40430 ± 0.00050	9.11	9.26	9.44	1.35	2.39	3.79	−0.039 ± 0.089	1.716 ± 1.330	0.2246 ± 0.2238
6936	2005jl	323.2338867188	−0.7000573874	0.18100 ± 0.00050	10.18	10.26	10.33	3.40	4.90	6.68	−0.011 ± 0.027	−0.144 ± 0.315	−0.0136 ± 0.0735
7143	2005jg	345.2623596191	−0.2068603635	0.30400 ± 0.00500	10.30	10.36	10.40	3.49	5.09	6.24	0.033 ± 0.040	−0.894 ± 0.590	−0.0097 ± 0.1264
7512	2005jo	52.0903663635	−0.3261369467	0.21900 ± 0.00500	−99.00	8.62	8.67	2.22	2.26	2.43	0.013 ± 0.031	0.279 ± 0.425	0.0395 ± 0.1191
7847	2005jp	32.4597015381	−0.0616886541	0.21240 ± 0.00050	10.43	10.49	10.58	3.28	4.25	7.31	0.174 ± 0.030	0.255 ± 0.410	−0.1968 ± 0.0875
8030	2005jv	40.2087211609	0.9932332635	0.42200 ± 0.00500	9.41	9.56	9.72	1.30	2.35	3.95	−0.165 ± 0.082	0.923 ± 1.127	0.3907 ± 0.2467
8213	2005ko	357.5210571289	−0.9214569926	0.18470 ± 0.00050	10.38	10.45	10.49	4.35	5.97	7.09	0.216 ± 0.040	−0.651 ± 0.377	−0.1624 ± 0.0913
8598	2005jt	42.6674690247	−0.0667039678	0.36060 ± 0.00050	10.01	10.11	10.19	1.63	2.11	2.73	0.090 ± 0.085	−1.283 ± 0.940	−0.3454 ± 0.2274
8719	2005kp	7.7218842506	−0.7186533809	0.11780 ± 0.00050	9.01	9.10	9.14	2.92	3.46	3.54	−0.099 ± 0.026	−0.263 ± 0.259	0.0664 ± 0.0649
9207	2005lg	19.0833320618	−0.8073787689	0.35000 ± 0.00050	10.73	10.79	10.85	4.10	5.26	5.99	0.002 ± 0.066	1.512 ± 0.916	0.0289 ± 0.1974
9457	2005li	335.8146362305	0.2536900640	0.25690 ± 0.00050	11.00	11.05	11.10	7.67	8.77	10.27	0.001 ± 0.065	−0.186 ± 0.819	−0.0116 ± 0.1659
10550	2005lf	349.6758117676	−1.2046753168	0.30010 ± 0.00050	10.33	10.38	10.39	1.77	1.80	3.26	0.068 ± 0.075	1.281 ± 1.130	0.1359 ± 0.2309
12781	2006er	5.4078617096	−1.0106090307	0.08431 ± 0.00016	10.96	10.97	11.02	10.58	11.18	11.58	0.072 ± 0.061	−2.128 ± 0.337	0.1604 ± 0.1149
12843	2006fa	323.8784790039	−0.9796369672	0.16704 ± 0.00013	11.18	11.22	11.28	7.61	8.71	10.61	0.082 ± 0.043	−1.110 ± 0.405	−0.3135 ± 0.1016
12856	2006fl	332.8653564453	0.7555990219	0.17173 ± 0.00011	10.32	10.37	10.45	3.16	3.93	6.07	−0.130 ± 0.023	0.738 ± 0.310	0.0908 ± 0.0711
12860	2006fc	323.6949768066	1.1754231453	0.12170 ± 0.00050	10.58	10.63	10.67	3.43	5.02	6.17	0.186 ± 0.024	−0.494 ± 0.258	−0.0007 ± 0.0649
12898	2006fw	26.7930507660	−0.1468682140	0.08350 ± 0.00050	9.96	9.97	10.01	6.93	7.65	8.43	0.074 ± 0.019	−0.332 ± 0.139	0.0141 ± 0.0583
12930	2006ex	309.6826477051	−0.4763843715	0.14749 ± 0.00017	10.85	10.88	10.90	4.12	4.61	5.12	−0.023 ± 0.037	1.623 ± 0.477	0.1716 ± 0.0947
12950	2006fy	351.6672668457	−0.8406041265	0.08268 ± 0.00004	9.75	9.78	9.81	3.18	3.81	4.34	0.028 ± 0.014	−0.731 ± 0.112	0.0301 ± 0.0480
12972	2006ft	7.9585695267	−0.3830518126	0.26080 ± 0.00050	9.12	9.18	9.27	2.06	2.67	3.83	−0.059 ± 0.044	0.723 ± 0.696	0.1218 ± 0.1387
13044	2006fm	332.5429992676	0.5039222836	0.12570 ± 0.00050	9.66	9.70	9.76	3.30	4.12	5.72	−0.083 ± 0.021	−0.197 ± 0.204	0.0565 ± 0.0547
13070	2006fu	357.7849121094	−0.7465677261	0.19855 ± 0.00009	10.18	10.22	10.23	3.08	3.74	4.13	−0.179 ± 0.027	0.717 ± 0.323	0.0957 ± 0.0754
13305	2006he	331.1001586914	0.6907849908	0.21390 ± 0.00050	10.01	10.06	10.11	2.58	3.50	4.63	−0.022 ± 0.030	1.020 ± 0.352	0.0304 ± 0.0817
13354	2006hr	27.5647277832	−0.8866921663	0.15760 ± 0.00010	10.46	10.51	10.56	3.59	4.73	6.74	0.087 ± 0.024	0.952 ± 0.225	−0.0979 ± 0.0592
13411	...	315.1897277832	0.1917154342	0.16300 ± 0.00050	9.13	9.21	9.29	3.74	5.40	6.90	−0.026 ± 0.034	1.191 ± 0.397	0.1275 ± 0.0895
13425	2006gp	338.5414733887	0.0548623651	0.21290 ± 0.00050	10.22	10.29	10.36	5.72	8.28	10.19	0.298 ± 0.054	−0.751 ± 0.579	−0.0301 ± 0.1606
13506	2006hg	25.2436542511	−0.7284323573	0.24500 ± 0.00050	10.13	10.18	10.22	2.35	3.93	5.25	0.165 ± 0.038	0.079 ± 0.582	0.0435 ± 0.1271
13511	2006hh	40.6112861633	−0.7942346931	0.23757 ± 0.00015	11.26	11.41	11.47	4.98	7.34	8.03	−0.092 ± 0.044	−1.991 ± 0.438	0.1846 ± 0.1132
13578	2006hc	17.3948116302	0.7042742372	0.22900 ± 0.00050	9.11	9.19	9.29	2.36	3.33	4.79	−0.043 ± 0.029	0.150 ± 0.464	0.1010 ± 0.1018
13641	2006hf	345.2174987793	−0.9820173383	0.21930 ± 0.00050	9.15	9.25	9.34	2.79	4.10	6.12	−0.046 ± 0.029	0.967 ± 0.322	−0.0431 ± 0.0777
13736	2006hv	336.8327026367	1.0307192802	0.15040 ± 0.00050	9.51	9.56	9.61	2.93	3.84	5.51	−0.040 ± 0.023	0.947 ± 0.232	0.0361 ± 0.0597
13757	2006hk	350.1237792969	−1.1580305099	0.28900 ± 0.00500	9.13	9.24	9.36	1.98	2.98	4.49	−0.203 ± 0.039	0.724 ± 0.416	0.1401 ± 0.1212
13796	2006hl	350.6919860840	0.5323168635	0.14820 ± 0.00050	10.16	10.22	10.27	4.41	5.99	7.12	−0.054 ± 0.021	0.518 ± 0.181	−0.0995 ± 0.0545
13835	2006hp	6.0593752861	−0.2492461652	0.24770 ± 0.00050	10.39	10.44	10.48	2.24	3.22	3.92	−0.064 ± 0.031	0.707 ± 0.295	0.0003 ± 0.0836
13894	2006jh	1.6905879974	−0.0367476977	0.12490 ± 0.00050	9.34	9.39	9.44	4.09	6.15	7.58	0.186 ± 0.022	0.446 ± 0.201	0.1657 ± 0.0547

Table 2
(Continued)

Designation		Host Coordinates		Redshift[a]	$M-$	M	$M+$	Age$-$	Age	Age+	c	x_1	HR
SN ID	IAU	$\alpha(J2000)$	$\delta(J2000)$			($\log M_\odot$)			(Gyr)				(mag)
13934	2006jg	342.1104431152	−0.4351437390	0.33000 ± 0.00500	10.76	10.83	10.90	2.69	4.58	6.13	−0.079 ± 0.078	−0.914 ± 0.786	0.2149 ± 0.2178
13956	2006hi	20.9414615631	0.8162868619	0.26200 ± 0.00500	10.53	10.61	10.77	6.22	8.62	9.72	0.144 ± 0.069	−0.552 ± 1.204	0.6144 ± 0.2207
14019	2006ki	316.6423950195	−0.6486185193	0.21640 ± 0.00050	9.69	9.74	9.82	2.33	2.96	4.12	0.001 ± 0.041	−0.337 ± 0.389	0.3925 ± 0.1018
14108	2006hu	53.5947074890	−1.1231447458	0.13300 ± 0.00500	8.77	8.86	8.96	3.53	4.83	6.79	−0.001 ± 0.020	0.053 ± 0.164	0.2947 ± 0.1352
14212	2006iy	330.4706420898	1.0444601774	0.20540 ± 0.00050	10.27	10.35	10.42	4.58	6.55	8.01	−0.009 ± 0.023	−0.415 ± 0.205	0.0090 ± 0.0620
14261	2006jk	328.2404174805	0.2536858320	0.28580 ± 0.00050	9.39	9.44	9.52	1.85	1.91	2.52	−0.037 ± 0.039	0.523 ± 0.543	−0.1989 ± 0.1132
14298	2006jj	314.8951110840	1.2232679129	0.27010 ± 0.00050	9.28	9.41	9.54	2.50	3.92	5.77	−0.085 ± 0.039	1.049 ± 0.442	0.0262 ± 0.1084
14331	2006kl	7.8891010284	−0.1355372667	0.22110 ± 0.00050	9.57	9.61	9.66	2.30	2.78	3.45	0.002 ± 0.033	−0.140 ± 0.313	0.1347 ± 0.0875
14397	2006kk	6.9156045914	0.6493207216	0.38570 ± 0.00050	10.55	10.61	10.71	1.98	2.59	4.17	−0.321 ± 0.083	−1.077 ± 0.745	0.4810 ± 0.2402
14437	2006hy	332.0809326172	−1.1963416338	0.14910 ± 0.00050	9.96	10.02	10.09	5.81	8.81	10.41	−0.106 ± 0.021	0.278 ± 0.192	−0.0850 ± 0.0544
14456	2006jm	343.5509338379	1.0508996248	0.33000 ± 0.00500	11.04	11.13	11.19	4.39	5.67	6.97	0.001 ± 0.042	0.163 ± 0.549	−0.2071 ± 0.1369
14481	2006lj	2.6814725399	0.2018533349	0.24390 ± 0.00050	10.96	11.08	11.17	4.92	8.95	8.95	−0.168 ± 0.050	−1.208 ± 0.443	0.3927 ± 0.1344
14735	2006km	35.1584739685	0.3481049836	0.30110 ± 0.00050	10.29	10.38	10.47	2.91	4.41	5.72	0.045 ± 0.039	0.157 ± 0.407	−0.2168 ± 0.1067
14782	2006jp	314.2340698242	−0.2791627347	0.16040 ± 0.00050	11.13	11.26	11.35	4.80	7.28	9.68	0.011 ± 0.023	−0.503 ± 0.211	−0.4487 ± 0.0597
14815	2006iz	319.0716552734	0.5595042109	0.13630 ± 0.00050	8.78	8.79	8.82	2.74	2.74	2.79	−0.027 ± 0.042	3.869 ± 0.430	0.2070 ± 0.1037
14846	2006jn	7.6626000404	0.1420275271	0.22470 ± 0.00050	10.96	10.99	11.04	4.23	5.68	6.97	−0.059 ± 0.030	0.378 ± 0.333	0.0229 ± 0.0894
14871	2006jq	54.2769241333	0.0092711495	0.12760 ± 0.00050	9.21	9.26	9.31	2.85	3.84	5.27	−0.086 ± 0.019	1.128 ± 0.178	0.0349 ± 0.0518
14979	2006jr	54.9465255737	0.9921327233	0.17710 ± 0.00050	10.00	10.01	10.10	3.96	4.42	6.78	−0.119 ± 0.021	−0.055 ± 0.192	−0.0599 ± 0.0596
15132	2006jt	329.6999511719	0.1987692863	0.14400 ± 0.00500	9.45	9.46	9.47	2.69	2.69	2.74	−0.138 ± 0.021	0.752 ± 0.211	0.1824 ± 0.1300
15201	2006ks	337.5189208984	0.0031410647	0.20850 ± 0.00050	11.26	11.34	11.41	6.16	8.16	10.26	0.129 ± 0.038	−1.386 ± 0.474	0.3592 ± 0.1117
15203	2006jy	15.7347574234	0.1830275059	0.20430 ± 0.00050	10.14	10.22	10.26	5.21	8.21	9.81	0.001 ± 0.028	1.139 ± 0.335	−0.0040 ± 0.0797
15213	2006lk	53.0192298889	−0.1002237424	0.31120 ± 0.00050	10.58	10.62	10.67	4.67	5.82	6.52	−0.042 ± 0.051	−0.247 ± 0.570	−0.1117 ± 0.1401
15217	2006jv	22.6341056824	0.2209988385	0.36800 ± 0.00500	10.71	10.79	10.87	3.80	4.77	6.65	−0.056 ± 0.116	−1.623 ± 1.142	−0.0224 ± 0.3205
15219	2006ka	34.6107521057	0.2261287570	0.24800 ± 0.00500	10.94	11.02	11.08	2.51	3.62	5.48	−0.165 ± 0.034	−0.294 ± 0.522	0.1063 ± 0.1252
15229	2006kr	4.8320274353	1.0906258821	0.22680 ± 0.00050	9.09	9.12	9.18	2.17	2.27	2.89	−0.048 ± 0.032	0.575 ± 0.362	0.0729 ± 0.0912
15259	2006kc	337.5441894531	−0.4077875614	0.21003 ± 0.00011	9.14	9.25	9.36	3.00	4.82	6.66	−0.005 ± 0.027	0.184 ± 0.290	−0.1254 ± 0.0775
15287	2006kt	323.9606628418	−1.0589238405	0.25400 ± 0.00500	10.47	10.58	10.65	4.30	6.70	8.85	−0.080 ± 0.027	0.859 ± 0.350	0.0237 ± 0.1050
15354	2006lp	6.7742686272	−0.1259586960	0.22210 ± 0.00050	10.82	10.85	10.88	9.02	10.12	11.02	0.138 ± 0.056	−2.119 ± 0.458	−0.1773 ± 0.1401
15356	2006lm	335.0533142090	0.4099416137	0.27470 ± 0.00050	10.41	10.54	10.62	4.62	6.72	8.65	−0.018 ± 0.046	−0.566 ± 0.530	−0.1923 ± 0.1300
15369	2006ln	348.8330383301	−0.5626841784	0.23200 ± 0.00500	8.95	9.06	9.18	2.72	4.02	5.83	−0.014 ± 0.026	0.624 ± 0.304	−0.4142 ± 0.1023
15383	2006lq	34.1496849060	−0.1552789956	0.31620 ± 0.00050	10.54	10.67	10.77	3.71	5.22	8.11	−0.042 ± 0.049	−0.332 ± 0.622	−0.0459 ± 0.1512
15421	2006kw	33.7412719727	0.6027206182	0.18500 ± 0.00050	10.09	10.14	10.22	3.01	4.10	5.68	−0.031 ± 0.024	−0.104 ± 0.297	0.0667 ± 0.0691
15425	2006kx	55.5610733032	0.4783548415	0.16004 ± 0.00014	10.50	10.57	10.59	4.69	6.29	8.69	−0.031 ± 0.021	0.834 ± 0.257	−0.2347 ± 0.0592
15440	2006lr	39.7205924988	0.0901087895	0.26190 ± 0.00050	10.59	10.71	10.83	3.76	6.23	7.80	0.097 ± 0.038	−0.767 ± 0.546	−0.2466 ± 0.1116
15443	2006lb	49.8674354553	−0.3179923296	0.18202 ± 0.00010	10.26	10.32	10.37	4.38	6.51	7.36	−0.077 ± 0.025	1.357 ± 0.304	−0.0756 ± 0.0592
15453	2006ky	319.6684570312	−1.0242410898	0.18370 ± 0.00050	8.95	9.04	9.14	3.08	4.53	6.17	−0.021 ± 0.031	1.279 ± 0.390	0.1745 ± 0.0757
15456	2006ll	331.8668518066	−0.9038056135	0.38210 ± 0.00050	10.93	10.97	11.02	5.08	5.76	6.15	−0.128 ± 0.083	−0.712 ± 1.053	−0.1778 ± 0.2437
15459	2006la	340.7014160156	−0.9017586112	0.12670 ± 0.00050	9.04	9.04	9.06	2.81	2.81	2.86	0.138 ± 0.026	0.225 ± 0.257	0.4487 ± 0.0599
15461	2006kz	326.8482055664	−0.4947634041	0.18000 ± 0.00500	10.30	10.35	10.42	4.82	6.09	8.25	−0.083 ± 0.027	−0.371 ± 0.280	−0.0081 ± 0.1148
15466	2006mz	317.6454467773	−0.1227247939	0.24610 ± 0.00050	10.50	10.56	10.61	2.53	3.93	5.74	0.070 ± 0.051	−1.494 ± 0.462	−0.3856 ± 0.1195
15467	...	320.0201110840	−0.1773548573	0.21043 ± 0.00009	10.35	10.35	10.37	2.27	2.31	2.85	−0.042 ± 0.032	0.848 ± 0.391	−0.1144 ± 0.0815
15504	2006oc	345.7013854980	−0.8768699169	0.27010 ± 0.00050	11.03	11.08	11.14	3.15	4.20	6.06	0.257 ± 0.061	3.638 ± 0.866	0.0931 ± 0.1800
15508	2006ls	27.1694507599	−0.5757497549	0.14740 ± 0.00050	9.85	9.88	9.91	2.80	3.39	3.96	−0.084 ± 0.021	0.574 ± 0.217	−0.1928 ± 0.0516
15583	2006mv	37.7310752869	0.9462816715	0.17520 ± 0.00050	9.08	9.13	9.19	2.74	3.24	4.44	0.069 ± 0.029	−0.474 ± 0.282	−0.0197 ± 0.0714
15648	2006ni	313.7187805176	−0.1958119273	0.17496 ± 0.00017	11.23	11.29	11.36	6.12	8.62	10.62	0.186 ± 0.049	−1.277 ± 0.511	−0.0871 ± 0.1083
15704	2006nh	40.2121353149	0.6598128676	0.36500 ± 0.00500	10.78	10.83	10.88	5.94	6.89	7.17	−0.096 ± 0.066	0.706 ± 0.874	0.1095 ± 0.1858
15776	2006na	32.8302955627	−0.9981175065	0.30500 ± 0.00500	11.18	11.19	11.21	9.81	10.21	10.21	−0.116 ± 0.081	−1.662 ± 0.743	0.1115 ± 0.2089
15872	2006nb	36.7223777771	−0.3278448582	0.18460 ± 0.00050	9.52	9.58	9.64	3.07	4.35	6.38	−0.027 ± 0.035	0.791 ± 0.460	0.0956 ± 0.0857
15897	2006pb	11.6815948486	−1.0324945450	0.17470 ± 0.00050	10.70	10.78	10.87	7.12	8.12	10.12	0.073 ± 0.052	−2.887 ± 0.338	−0.1306 ± 0.1019
15901	2006od	31.9762687683	−0.5353427529	0.20530 ± 0.00050	9.84	9.92	10.00	3.36	4.70	6.22	−0.079 ± 0.030	−0.420 ± 0.332	0.0116 ± 0.0756
16000	2006nj	21.1174659729	0.0743126571	0.39000 ± 0.00500	9.26	9.41	9.57	1.42	2.29	4.15	−0.163 ± 0.072	1.448 ± 1.091	0.3161 ± 0.1916
16072	2006nv	3.1245520115	−0.9778423309	0.28670 ± 0.00050	10.80	10.83	10.96	4.51	5.49	8.52	−0.044 ± 0.049	0.058 ± 0.691	−0.0728 ± 0.1285
16073	2006of	8.1076574326	−1.0539033413	0.15310 ± 0.00050	9.68	9.73	9.78	3.62	5.08	6.40	−0.018 ± 0.017	0.080 ± 0.252	0.1098 ± 0.0516
16099	2006nn	26.4212512970	−1.0545672178	0.19686 ± 0.00015	10.49	10.55	10.61	4.66	6.29	7.72	0.004 ± 0.025	1.934 ± 0.581	0.1190 ± 0.0855
16100	2006nl	30.4363574982	−1.0323493481	0.19500 ± 0.00500	9.32	9.42	9.50	4.90	7.41	9.90	0.097 ± 0.033	−0.355 ± 0.451	0.0264 ± 0.1237
16106	2006no	332.0898742676	−1.1483064890	0.25120 ± 0.00050	10.80	10.92	10.98	3.73	4.33	7.33	−0.115 ± 0.044	−0.167 ± 0.629	−0.0047 ± 0.1344
16185	2006ok	16.8680858612	−0.2693305314	0.09700 ± 0.00500	9.59	9.64	9.69	6.42	8.58	9.56	0.178 ± 0.031	−1.614 ± 0.277	0.1008 ± 0.1850
16232	2006oj	17.2049808502	−0.9894958138	0.36700 ± 0.00500	10.54	10.62	10.70	2.99	5.00	5.93	−0.117 ± 0.082	−0.246 ± 0.862	0.0913 ± 0.1821
17168	2007ik	339.7236328125	−1.1672555208	0.18400 ± 0.00500	9.46	9.50	9.54	2.54	2.81	3.61	−0.016 ± 0.034	0.280 ± 0.382	0.0588 ± 0.1338
17332	2007jk	43.7725067139	−0.1476856470	0.18284 ± 0.00015	10.43	10.55	10.64	3.91	6.66	8.68	0.088 ± 0.032	−0.254 ± 0.314	−0.1682 ± 0.0947
17366	2007hz	315.7849731445	−1.0311613083	0.13933 ± 0.00017	10.87	10.92	10.97	3.74	5.18	6.74	−0.125 ± 0.025	0.588 ± 0.253	−0.0077 ± 0.0689
17389	2007ih	323.2950134277	−0.9600833058	0.17060 ± 0.00050	9.82	9.90	9.97	3.68	4.99	6.84	0.063 ± 0.033	1.104 ± 0.406	0.2739 ± 0.1036
17497	2007jt	37.1364936829	−1.0428131819	0.14478 ± 0.00010	10.33	10.39	10.43	2.98	3.91	4.63	0.057 ± 0.020	0.596 ± 0.180	−0.1025 ± 0.0510
17552	2007jl	322.3212585449	−1.0028200150	0.25420 ± 0.00050	10.55	10.61	10.66	2.10	3.36	5.19	−0.016 ± 0.039	0.766 ± 0.403	0.0018 ± 0.1132
17568	2007kb	313.1032714844	0.2774721682	0.14450 ± 0.00050	9.93	10.00	10.06	3.70	5.30	7.06	0.265 ± 0.041	0.626 ± 0.367	0.4458 ± 0.0968
17629	2007jw	30.6364746094	−1.0899255276	0.13690 ± 0.00007	11.07	11.13	11.13	5.64	7.92	8.67	0.084 ± 0.028	−0.502 ± 0.213	−0.1519 ± 0.0665
17745	2007ju	2.9602687359	−0.3393539488	0.06360 ± 0.00050	8.87	8.88	8.89	3.26	3.26	3.33	−0.056 ± 0.028	0.882 ± 0.274	0.0199 ± 0.0981
17791	2007kp	332.3733825684	0.7380061746	0.28620 ± 0.00050	9.30	9.38	9.48	1.99	2.78	3.82	−0.214 ± 0.068	−0.372 ± 0.768	0.5136 ± 0.1888
17801	2007ko	316.0938110352	−0.8984486461	0.20640 ± 0.00050	11.26	11.34	11.44	4.31	6.29	7.63	0.029 ± 0.049	−0.306 ± 0.554	0.2287 ± 0.1241
17809	2007kr	6.3649182320	−0.8392885327	0.28200 ± 0.00500	9.66	9.72	9.79	2.02	2.55	3.62	0.033 ± 0.037	1.674 ± 0.499	−0.0922 ± 0.1303
17811	2007ix	12.8806476593	−0.9462078214	0.21320 ± 0.00050	9.97	10.10	10.21	5.71	8.21	10.21	−0.150 ± 0.030	0.817 ± 0.365	−0.0017 ± 0.0966
17875	2007jz	20.9837265015	1.2550705671	0.23230 ± 0.00050	10.50	10.62	10.69	4.49	6.49	7.77	−0.086 ± 0.038	0.753 ± 0.338	0.1205 ± 0.0983
17884	2007kt	27.5993213654	1.1723767519	0.23900 ± 0.00500	10.20	10.24	10.28	4.50	6.02	7.32	−0.147 ± 0.036	0.179 ± 0.378	−0.0219 ± 0.1186

Table 2
(Continued)

Designation		Host Coordinates		Redshift[a]	$M-$	M	$M+$	Age$-$	Age	Age+	c	x_1	HR
SN ID	IAU	$\alpha(J2000)$	$\delta(J2000)$			($\log M_\odot$)			(Gyr)				(mag)
18091	2007ku	23.3678874969	0.5246205926	0.37160 ± 0.00050	11.00	11.03	11.07	4.99	5.14	5.64	-0.189 ± 0.070	-0.021 ± 0.777	0.1106 ± 0.1888
18241	2007ks	312.3875427246	−0.7619610429	0.09500 ± 0.01000	9.42	9.48	9.55	3.71	5.52	7.12	-0.080 ± 0.035	-1.273 ± 0.195	0.1971 ± 0.3543
18323	2007kx	3.4286384583	0.6523273587	0.15460 ± 0.00050	9.32	9.37	9.44	3.61	4.76	6.39	-0.059 ± 0.029	-0.270 ± 0.284	0.1280 ± 0.0778
18375	2007lg	11.5163803101	−0.0106749199	0.11040 ± 0.00050	10.30	10.43	10.50	4.64	6.60	7.70	0.057 ± 0.019	0.861 ± 0.163	-0.1803 ± 0.0521
18415	2007la	337.4775085449	1.0584667921	0.13070 ± 0.00050	10.90	10.98	11.05	6.02	8.02	10.15	-0.034 ± 0.041	-2.093 ± 0.287	-0.0752 ± 0.0897
18485	2007nu	47.9590339661	−0.6926384568	0.28200 ± 0.00050	10.72	10.78	10.83	4.79	6.06	6.73	-0.072 ± 0.038	1.323 ± 0.474	-0.0585 ± 0.1116
18486	2007ln	55.1812210083	1.0045801401	0.24030 ± 0.00060	9.41	9.50	9.58	2.96	4.61	6.28	-0.109 ± 0.029	1.008 ± 0.323	-0.1315 ± 0.0817
18602	2007lo	338.9836730957	0.6091071367	0.13840 ± 0.00050	9.20	9.27	9.34	3.39	4.89	6.59	0.068 ± 0.027	0.812 ± 0.254	0.0493 ± 0.0623
18604	2007lp	340.9206848145	0.4205097556	0.17610 ± 0.00050	11.04	11.10	11.17	7.11	9.11	10.51	0.004 ± 0.035	-2.395 ± 0.271	0.1204 ± 0.0818
18612	2007lc	12.2880029678	0.5966250896	0.11504 ± 0.00015	11.05	11.05	11.07	5.86	7.15	8.90	0.069 ± 0.024	-1.218 ± 0.226	-0.1887 ± 0.0619
18617	2007mw	345.7612915039	0.8493407369	0.32820 ± 0.00050	9.83	9.93	10.02	2.50	3.80	5.23	-0.001 ± 0.060	-0.590 ± 0.805	-0.1412 ± 0.1913
18650	2007lt	328.4472045898	0.0150281759	0.11300 ± 0.00500	8.86	8.91	8.93	2.90	3.05	3.71	-0.076 ± 0.023	0.821 ± 0.223	0.2338 ± 0.1552
18721	2007mu	3.0777626038	−0.0776401758	0.40309 ± 0.00018	11.16	11.17	11.24	4.73	5.64	6.59	-0.098 ± 0.074	0.569 ± 0.931	-0.0820 ± 0.2083
18749	2007mb	12.5465755463	0.6757113338	0.18940 ± 0.00050	11.14	11.20	11.23	7.96	9.36	9.96	0.096 ± 0.040	-1.780 ± 0.477	-0.1039 ± 0.1069
18751	2007ly	5.7224216461	0.7759432793	0.07130 ± 0.00050	10.10	10.12	10.14	9.74	11.34	12.34	0.478 ± 0.077	-1.967 ± 0.510	0.2231 ± 0.2149
18782	2007ns	39.2622032166	−0.8667251468	0.36590 ± 0.00050	10.94	11.10	11.14	3.81	5.01	5.93	-0.275 ± 0.075	-0.655 ± 0.838	0.3879 ± 0.1999
18890	2007mm	16.4433784485	−0.7594780922	0.06643 ± 0.00016	10.20	10.28	10.34	6.06	7.80	8.20	0.399 ± 0.061	-2.995 ± 0.288	0.1322 ± 0.1316
18927	2007nt	46.6823501587	−0.7540850639	0.21290 ± 0.00050	10.40	10.46	10.51	5.42	7.31	8.49	0.159 ± 0.035	-0.834 ± 0.389	-0.2880 ± 0.1001
18940	2007sb	10.3486833572	0.4118011594	0.21230 ± 0.00050	10.17	10.23	10.28	3.33	4.51	5.97	-0.003 ± 0.031	-0.878 ± 0.318	-0.0743 ± 0.0837
18945	2007nd	10.0779104233	−1.0390836000	0.26330 ± 0.00050	9.61	9.67	9.75	2.23	3.19	4.46	-0.033 ± 0.037	-0.088 ± 0.579	0.1640 ± 0.1179
18965	2007ne	13.5092248917	1.0689095259	0.20660 ± 0.00050	10.37	10.47	10.53	3.78	4.31	5.78	-0.124 ± 0.037	-1.310 ± 0.353	-0.0385 ± 0.0875
19002	2007nh	42.6161956787	−0.5511860251	0.26290 ± 0.00050	10.68	10.84	10.95	2.81	4.96	6.83	-0.097 ± 0.029	0.263 ± 0.380	-0.0021 ± 0.0836
19008	2007mz	331.9632873535	−1.0700660944	0.23220 ± 0.00050	10.40	10.46	10.50	2.64	3.95	5.60	0.089 ± 0.038	1.210 ± 0.478	-0.1803 ± 0.1001
19027	2007my	328.8840332031	−0.3717949390	0.29320 ± 0.00050	9.42	9.43	9.46	1.81	1.83	1.87	0.006 ± 0.044	0.217 ± 0.608	-0.4353 ± 0.1387
19029	2007lu	330.3953247070	−0.2568780780	0.31950 ± 0.00050	9.70	9.73	9.78	1.67	1.70	2.24	-0.127 ± 0.088	3.565 ± 0.996	0.7472 ± 0.2665
19033	2007of	316.2346191406	0.0608703010	0.40470 ± 0.00050	10.01	10.11	10.21	1.89	3.03	4.48	-0.092 ± 0.090	0.693 ± 1.215	0.2684 ± 0.2699
19067	2007oq	325.6280822754	0.9846492410	0.33910 ± 0.00050	9.67	9.80	9.91	2.71	4.48	5.82	0.016 ± 0.059	2.872 ± 1.342	-0.0072 ± 0.2755
19149	2007ni	31.4603996277	−0.3325760365	0.19600 ± 0.00500	9.45	9.49	9.54	2.46	3.00	3.62	0.078 ± 0.027	1.492 ± 0.329	-0.3660 ± 0.1133
19174	2007or	25.6597671509	1.0303381681	0.16640 ± 0.00050	11.03	11.06	11.10	8.62	10.22	10.72	0.074 ± 0.032	-1.088 ± 0.305	-0.2163 ± 0.0798
19211	2007oh	313.1539306641	−0.4541013539	0.41990 ± 0.00050	10.29	10.40	10.52	2.10	3.73	5.51	-0.107 ± 0.087	0.702 ± 1.220	0.2239 ± 0.2425
19230	2007mo	332.8909912109	0.7647492290	0.22150 ± 0.00050	10.32	10.42	10.47	4.03	6.03	8.63	0.145 ± 0.050	-1.493 ± 0.581	-0.3277 ± 0.1387
19282	2007mk	359.0729980469	−0.5038936734	0.18641 ± 0.00016	8.54	8.59	8.64	2.42	2.46	3.00	-0.107 ± 0.023	0.530 ± 0.279	-0.0657 ± 0.0593
19341	2007nf	15.8608398438	0.3316199183	0.22800 ± 0.00500	10.99	11.03	11.07	7.96	9.96	10.58	0.071 ± 0.052	-1.940 ± 0.488	-0.1392 ± 0.1435
19353	2007nj	43.1132774353	0.2517381907	0.15395 ± 0.00011	10.83	10.86	10.86	6.77	8.50	8.50	0.059 ± 0.023	0.863 ± 0.308	-0.0349 ± 0.0665
19425	2007ow	323.5083923340	−0.7406359315	0.21160 ± 0.00050	10.53	10.60	10.68	5.13	8.23	10.13	0.210 ± 0.060	-1.419 ± 0.558	-0.0122 ± 0.1373
19543	2007oj	357.9083862305	0.2798276842	0.12300 ± 0.00500	8.78	8.84	8.90	3.16	4.03	5.30	-0.007 ± 0.026	-1.104 ± 0.235	0.1811 ± 0.1463
19596	2007po	53.8846893311	0.7037985921	0.29200 ± 0.00500	9.69	9.78	9.88	2.38	3.50	4.94	-0.033 ± 0.042	0.986 ± 0.638	0.0210 ± 0.1451
19604	2007oi	5.3261027336	1.0737973452	0.29600 ± 0.00500	10.07	10.17	10.25	2.51	4.26	6.08	0.172 ± 0.068	1.950 ± 1.012	0.3947 ± 0.2209
19626	2007ou	35.9277305603	−0.8264662623	0.11321 ± 0.00005	10.27	10.30	10.36	3.71	4.73	6.24	0.329 ± 0.034	1.744 ± 0.461	0.4453 ± 0.0815
19632	2007ov	40.2866287231	0.1442469060	0.31530 ± 0.00050	10.97	11.06	11.15	4.25	7.12	8.72	-0.025 ± 0.046	-0.052 ± 0.596	-0.0682 ± 0.1344
19658	2007ot	8.9032306671	−0.2325988412	0.20000 ± 0.00050	8.72	8.78	8.87	2.37	2.97	4.12	-0.093 ± 0.030	-0.401 ± 0.350	0.0771 ± 0.0756
19757	2007oy	349.4814147949	1.2236189842	0.40300 ± 0.00500	10.26	10.39	10.56	1.98	3.51	5.47	-0.087 ± 0.087	0.144 ± 1.079	-0.3474 ± 0.2605
19775	2007pc	318.9561462402	0.6512132883	0.13790 ± 0.00050	10.78	10.88	10.97	4.78	6.75	8.32	0.119 ± 0.027	-0.621 ± 0.314	-0.0728 ± 0.0694
19794	2007oz	359.3190917969	0.2484871745	0.29730 ± 0.00018	11.16	11.41	11.44	4.28	9.38	9.88	0.068 ± 0.094	-2.117 ± 0.938	0.0166 ± 0.2460
19818	2007pe	35.2665252686	0.4965370297	0.30440 ± 0.00050	10.14	10.22	10.30	2.54	4.19	5.54	-0.056 ± 0.040	0.613 ± 0.556	-0.2044 ± 0.1116
19913	2007qf	333.7622070312	−0.3417298794	0.20380 ± 0.00050	9.79	9.83	9.85	2.41	2.89	3.57	-0.056 ± 0.028	0.245 ± 0.457	0.1322 ± 0.0856
19940	2007pa	315.3935546875	−0.2687674761	0.15710 ± 0.00080	8.74	8.85	8.98	3.26	4.60	6.59	0.019 ± 0.025	1.099 ± 0.340	-0.3307 ± 0.0676
19969	2007pt	31.9098148346	−0.3240273297	0.17529 ± 0.00010	10.31	10.32	10.34	2.49	2.53	3.07	0.034 ± 0.025	-0.485 ± 0.345	-0.1577 ± 0.0711
19990	2007ps	34.8060150146	−0.3845337927	0.24600 ± 0.00500	10.52	10.59	10.64	6.38	8.78	10.38	-0.038 ± 0.044	-1.164 ± 0.491	0.0404 ± 0.1339
20040	2007rf	328.8794555664	0.8150795698	0.28800 ± 0.00050	10.27	10.38	10.47	3.97	6.37	8.53	-0.097 ± 0.046	0.829 ± 0.731	-0.1062 ± 0.1240
20048	2007pq	339.3081054688	0.7363132834	0.18550 ± 0.00050	10.71	10.80	10.87	7.01	8.01	11.01	0.050 ± 0.040	-0.939 ± 0.567	0.0230 ± 0.1211
20064	2007om	358.5862731934	−0.9172353745	0.10503 ± 0.00018	11.16	11.16	11.27	4.69	4.69	6.85	0.107 ± 0.023	0.408 ± 0.322	-0.2490 ± 0.0619
20106	2007pr	346.5540771484	0.3289288580	0.33300 ± 0.00500	10.12	10.20	10.26	3.05	5.27	6.52	-0.042 ± 0.084	-0.503 ± 0.905	0.0408 ± 0.2340
20111	2007pw	354.3940734863	0.2474300116	0.24500 ± 0.00500	10.78	10.87	10.93	5.90	8.39	8.94	0.015 ± 0.048	-0.362 ± 0.810	-0.0164 ± 0.1594
20184	2007qn	359.7885131836	1.1585552692	0.32400 ± 0.00050	9.53	9.65	9.75	2.21	3.38	4.62	0.029 ± 0.082	-1.095 ± 1.398	-0.2104 ± 0.2047
20227	2007qi	349.1200561523	−0.0988994613	0.27640 ± 0.00050	10.64	10.71	10.76	5.08	7.48	8.64	-0.134 ± 0.057	-1.647 ± 0.713	0.0382 ± 0.1498
20350	2007ph	312.8067932129	−0.9577776194	0.12946 ± 0.00018	11.19	11.29	11.34	5.03	8.14	9.63	0.213 ± 0.054	-3.029 ± 0.845	-0.0720 ± 0.1358
20364	2007qo	25.7565631866	−0.9451811910	0.21810 ± 0.00090	10.31	10.37	10.41	2.76	3.60	5.70	0.062 ± 0.039	0.830 ± 0.964	0.0192 ± 0.1404
20376	2007re	319.3955078125	−0.5239647627	0.21090 ± 0.00050	10.61	10.69	10.74	5.74	9.14	10.24	0.164 ± 0.045	-1.096 ± 0.874	-0.3531 ± 0.1499
20821	2007rk	55.5723648071	1.0622460842	0.19590 ± 0.00050	10.58	10.63	10.68	2.94	4.02	5.60	0.285 ± 0.057	-1.504 ± 1.272	0.0002 ± 0.2060

Note. [a] Redshift error $\geqslant 0.005$ corresponds to a redshift from the SN spectrum; redshift error $\leqslant 0.0005$ corresponds to a redshift from the host galaxy.

age,[17] and this in part may be why HRs are more strongly correlated with mass. Thus, the true underlying property influencing the SN Ia explosion is still unclear. The strength of both correlations may be improved by having UV and near-IR matches for all SDSS hosts and by calculating galaxy magnitudes in a consistent manner through matched apertures for all survey types (as was done, e.g., in Hill et al. 2011), ensuring that UV–optical–near-IR colors are accurate. It is also possible that the relationship between HR and age or mass is not simply linear and may be

[17] Our method yields uncertainties of 2% for mass and 27% for age, though we emphasize that these uncertainties are *statistical* only (as described in Section 3.3 and discussed in Section 4.4) and that systematic uncertainties on mass are around 0.1 dex (25%) at best. Running our linear regression on the HR-versus-mass plot with mass uncertainties inflated to be at least 0.1 dex does not change our results.

more complex. Additionally, in an ideal case of a well-resolved extended host, a local age computed from photometry obtained from the location of the SN in the galaxy would be preferable to the global galaxy average age that we compute here and would likely correlate more strongly with properties of the SN Ia.

We find that the HR trend with mass persists if we consider the subsample for which SDSS is complete. Therefore, based on our measurements and the completeness of our data set, it is likely that SNe Ia that are underluminous after light-curve correction do not occur in massive galaxies. This view is consistent with the results of Kasen et al. (2009) who showed using SN Ia simulations and the Timmes et al. (2003) model that metallicity can affect the explosion physics in such a way as to cause metal-rich progenitors to produce SNe Ia that are fast-declining and intrinsically fainter at peak. The usual light-curve correction technique does not account for this metallicity effect, and so metal-rich progenitors result in overluminous SNe Ia after corrections for light-curve shape. Thus, the Kasen et al. (2009) result is in agreement with the trends we see with mass (and, for the full sample, age) since galaxies with higher metallicity are, in general, older and more massive (Tremonti et al. 2004; Gallazzi et al. 2005).

Given our data set and the large scatter in our trends of HR with age and mass, it is not possible to determine for certain what host property most influences SN Ia luminosity. It is improbable that host mass itself, though better estimated, has a direct impact on SNe Ia. Rather, it is more likely that host mass is correlated with other properties of the host that do directly influence the progenitors of SNe Ia. The complexity of the relationships between galaxy properties such as age, mass, metallicity, dust, and SFR makes disentangling the factors that affect SNe Ia a challenge. Further study is needed to truly ascertain the origin of these correlations between host properties and Hubble residuals and to potentially pinpoint the cause of these observed trends.

We are grateful to Jennifer Mosher and John Fischer for their advice and suggestions. We also thank C. Jonathan MacDonald for his programming insight, Bernie Shiao (STScI) for his help with *GALEX* photometry, Steve Warren and Daniel Mortlock (UKIDSS) for their help in understanding the UKIDSS photometry, and Patrick Kelly for his assistance with linear fitting.

GALEX (*Galaxy Evolution Explorer*) is a NASA Small Explorer, launched in 2003 April. We gratefully acknowledge NASA's support for construction, operation, and science analysis for the *GALEX* mission, developed in cooperation with the Centre National d'Études Spatiales of France and the Korean Ministry of Science and Technology.

This work is based in part on data obtained as part of the UKIRT Infrared Deep Sky Survey (UKIDSS). The United Kingdom Infrared Telescope (UKIRT) is operated by the Joint Astronomy Centre on behalf of the Science and Technology Facilities Council of the UK.

Funding for the creation and distribution of the SDSS and SDSS-II has been provided by the Alfred P. Sloan Foundation, the Participating Institutions, the National Science Foundation, the U.S. Department of Energy, the National Aeronautics and Space Administration, the Japanese Monbukagakusho, the Max Planck Society, and the Higher Education Funding Council for England. The SDSS Web site is http://www.sdss.org/.

The SDSS is managed by the Astrophysical Research Consortium for the Participating Institutions. The Participating Institutions are the American Museum of Natural History, Astrophysical Institute Potsdam, University of Basel, Cambridge University, Case Western Reserve University, University of Chicago, Drexel University, Fermilab, the Institute for Advanced Study, the Japan Participation Group, Johns Hopkins University, the Joint Institute for Nuclear Astrophysics, the Kavli Institute for Particle Astrophysics and Cosmology, the Korean Scientist Group, the Chinese Academy of Sciences (LAMOST), Los Alamos National Laboratory, the Max-Planck-Institute for Astronomy (MPA), the Max-Planck-Institute for Astrophysics (MPIA), New Mexico State University, Ohio State University, University of Pittsburgh, University of Portsmouth, Princeton University, the United States Naval Observatory, and the University of Washington.

This work is based in part on observations made at the following telescopes. The Hobby–Eberly Telescope (HET) is a joint project of the University of Texas at Austin, the Pennsylvania State University, Stanford University, Ludwig-Maximilians-Universität München, and Georg-August-Universität Göttingen. The HET is named in honor of its principal benefactors, William P. Hobby and Robert E. Eberly. The Marcario Low-Resolution Spectrograph is named for Mike Marcario of High Lonesome Optics, who fabricated several optical elements for the instrument but died before its completion; it is a joint project of the Hobby–Eberly Telescope partnership and the Instituto de Astronomía de la Universidad Nacional Autónomade México. The Apache Point Observatory 3.5 m telescope is owned and operated by the Astrophysical Research Consortium. We thank the observatory director, Suzanne Hawley, and site manager, Bruce Gillespie, for their support of this project. The Subaru Telescope is operated by the National Astronomical Observatory of Japan. The William Herschel Telescope is operated by the Isaac Newton Group on the island of La Palma in the Spanish Observatorio del Roque de los Muchachos of the Instituto de Astrofisica de Canarias. The W. M. Keck Observatory is operated as a scientific partnership among the California Institute of Technology, the University of California, and the National Aeronautics and Space Administration; the observatory was made possible by the generous financial support of the W. M. Keck Foundation.

This work was funded by the NASA ADP Program NNX09AC75G.

Facilities: Sloan, *GALEX*, UKIRT

REFERENCES

Abazajian, K. N., Adelman-McCarthy, J. K., Ageros, M. A., et al. 2009, ApJS, 182, 543
Blanton, M. R., Brinkmann, J, Csabai, I., et al. 2003, AJ, 125, 2348
Bruzual, G., & Charlot, S. 2003, MNRAS, 344, 1000
Cardelli, J. A., Clayton, G. C., & Mathis, J. S. 1989, ApJ, 345, 245
Chabrier, G. 2003, PASP, 115, 763
Charlot, S., & Fall, S. M. 2000, ApJ, 539, 718
Conley, A., Sullivan, M., Hsiao, E. Y., et al. 2008, ApJ, 681, 482
Conroy, C., & Gunn, J. E. 2010, ApJ, 712, 833
Conroy, C., Gunn, J. E., & White, M. 2009, ApJ, 699, 486
Fioc, M., & Rocca-Volmerange, B. 1997, A&A, 326, 950
Frieman, J. A., Bassett, B., Becker, A., et al. 2008, AJ, 135, 338
Fukugita, M., Ichikawa, T., Gunn, J. E., et al. 1996, AJ, 111, 1748
Gallagher, J. S., Garnavich, P. M., Berlind, P., et al. 2005, ApJ, 634, 210
Gallagher, J. S., Garnavich, P. M., Caldwell, N., et al. 2008, ApJ, 685, 752
Gallazzi, A., Charlot, S., Brinchmann, J., White, S. D. M., & Tremonti, C. A. 2005, MNRAS, 362, 41
Gunn, J. E., Carr, M., Rockosi, C., et al. 1998, AJ, 116, 3040
Gunn, J. E., Siegmund, W. A., Mannery, E. J., et al. 2006, AJ, 131, 2332
Guy, J., Astier, P., Baumont, S., et al. 2007, A&A, 466, 11
Hamuy, M., Phillips, M. M., Maza, J., et al. 1995, AJ, 109, 1
Hamuy, M., Phillips, M. M., Suntzeff, N. B., et al. 1996a, AJ, 112, 2391
Hamuy, M., Phillips, M. M., Suntzeff, N. B., et al. 1996b, AJ, 112, 2398
Hamuy, M., Trager, S. C., Pinto, P. A., et al. 2000, AJ, 120, 1479

Hewett, P. C., Warren, S. J., Leggett, S. K., & Hodgkin, S. T. 2006, MNRAS, 367, 454
Hill, D. T., Kelvin, L. S., Driver, S. P., et al. 2011, MNRAS, 412, 765
Hillebrandt, W., & Niemeyer, J. C. 2000, ARA&A, 38, 191
Höflich, P., Wheeler, J. C., & Thielemann, F. K. 1998, ApJ, 495, 617
Holtzman, J. A., Marriner, J., Kessler, R., et al. 2008, AJ, 136, 2306
Howell, D. A., Sullivan, M., Brown, E. F., et al. 2009, ApJ, 691, 661
Jha, S., Riess, A. G., & Kirshner, R. P. 2007, ApJ, 659, 122
Kasen, D., Röpke, F. K., & Woosley, S. E. 2009, Nature, 460, 869
Kelly, B. C. 2007, ApJ, 665, 1489
Kelly, P. L., Hicken, M., Burke, D. L., Mandel, K. S., & Kirshner, R. P. 2010, ApJ, 715, 743
Kessler, R., Becker, A. C., Cinabro, D., et al. 2009a, ApJS, 185, 32
Kessler, R., Bernstein, J. P., Cinabro, D., et al. 2009b, PASP, 121, 1028
Kong, X., Charlot, S., Brinchmann, J., & Fall, S. M. 2004, MNRAS, 349, 769
Kron, R. G. 1980, ApJS, 43, 305
Lampeitl, H., Smith, M., Nichol, R. C., et al. 2010, ApJ, 722, 566
Lawrence, A., Warren, S. J., Almaini, O., et al. 2007, MNRAS, 379, 1599
Le Borgne, D., & Rocca-Volmerange, B. 2002, A&A, 386, 446
Lee, H.-c., Worthey, G., Trager, S. C., & Faber, S. M. 2007, ApJ, 664, 215
Mannucci, F., Della Valle, M., Panagia, N., et al. 2005, A&A, 433, 807
Marriner, J., et al. 2011, ApJ, in press
Martin, D. C., Fanson, J., Schiminovich, D., et al. 2005, ApJ, 619, L1
Neill, J. D., Sullivan, M., Howell, D. A., et al. 2009, ApJ, 707, 1449
Oke, J. B., & Gunn, J. E. 1983, ApJ, 266, 713
Perlmutter, S., Aldering, G., Goldhaber, G., et al. 1999, ApJ, 517, 565
Petrosian, V. 1976, ApJ, 209, L1
Phillips, M. M. 1993, ApJ, 413, L105
Riess, A. G., Filippenko, A. V., Challis, P., et al. 1998, AJ, 116, 1009
Riess, A. G., Press, W. H., & Kirshner, R. P. 1996, ApJ, 473, 88
Sako, M., Bassett, B., Becker, A., et al. 2008, AJ, 135, 348
Salim, S., Charlot, S., Rich, R. M., et al. 2005, ApJ, 619, L39
Schlegel, D. J., Finkbeiner, D. P., & Davis, M. 1998, ApJ, 500, 525
Smith, A. J., Loveday, L., & Cross, N. J. G. 2009, MNRAS, 397, 868
Sullivan, M., Conley, A., Howell, D. A., et al. 2010, MNRAS, 406, 782
Sullivan, M., Le Borgne, D., Pritchet, C. J., et al. 2006, ApJ, 648, 868
Timmes, F. X., Brown, E. F., & Truran, J. W. 2003, ApJ, 590, L83
Tremonti, C. A., Heckman, T. M., Kauffmann, G., et al. 2004, ApJ, 613, 898
van den Bergh, S. 1990, PASP, 102, 1318
Whelan, J., & Iben, I. J. 1973, ApJ, 186, 1007
York, D. G., Adelman, J., Anderson, J. E., Jr., et al. 2000, AJ, 120, 1579

The Astrophysical Journal, 741:127 (1pp), 2011 November 10 doi:10.1088/0004-637X/741/2/127

ERRATUM: "IMPROVED CONSTRAINTS ON TYPE Ia SUPERNOVA HOST GALAXY PROPERTIES USING MULTI-WAVELENGTH PHOTOMETRY AND THEIR CORRELATIONS WITH SUPERNOVA PROPERTIES" (2011, ApJ, 740, 92)

Ravi R. Gupta[1], Chris B. D'Andrea[1], Masao Sako[1], Charlie Conroy[2], Mathew Smith[3], Bruce Bassett[4,5,6], Joshua A. Frieman[7,8], Peter M. Garnavich[9], Saurabh W. Jha[10], Richard Kessler[7,11], Hubert Lampeitl[12], John Marriner[8], Robert C. Nichol[12], and Donald P. Schneider[13]
[1] Department of Physics and Astronomy, University of Pennsylvania, Philadelphia, PA 19104, USA; ravgupta@physics.upenn.edu
[2] Harvard-Smithsonian Center for Astrophysics, Cambridge, MA 02138, USA
[3] Astrophysics, Cosmology and Gravity Centre (ACGC), Department of Mathematics and Applied Mathematics, University of Cape Town, Rondebosch 7701, South Africa
[4] South African Astronomical Observatory, Observatory 7935, South Africa
[5] Department of Mathematics and Applied Mathematics, University of Cape Town, Rondebosch 7701, South Africa
[6] African Institute for Mathematical Sciences, Muizenberg, Cape Town, South Africa
[7] Department of Astronomy & Astrophysics, University of Chicago, Chicago, IL 60637, USA
[8] Fermilab, Batavia, IL 60510, USA
[9] Department of Physics, University of Notre Dame, Notre Dame, IN 46556, USA
[10] Department of Physics & Astronomy, Rutgers, the State University of New Jersey, Piscataway, NJ 08854, USA
[11] Kavli Institute for Cosmological Physics, The University of Chicago, Chicago, IL 60637, USA
[12] Institute of Cosmology and Gravitation, University of Portsmouth, Portsmouth, PO1 3FX, UK
[13] Department of Astronomy & Astrophysics, The Pennsylvania State University, University Park, PA 16802, USA
Received 2011 October 6; published 2011 October 25

Due to an error at the publisher, the following sentence in Section 2.2 was rendered incorrectly: "In order to match our SNe with host galaxies, we search the SDSS deep optical stacked images of Stripe 82 (Abazajian et al. 2009) for galaxies within a 0.″25 radius of the SN position, as was done by Lampeitl et al. (2010) and M. Smith et al. (2011, in preparation)." The correct radius should be in arcminutes (0.′25), not arcseconds. IOP Publishing sincerely regrets this error.

REFERENCES

Abazajian, K. N., Adelman-McCarthy, J. K., Ageros, M. A., et al. 2009, ApJS, 182, 543
Lampeitt, H., Smith, M., Nichol, R. C., et al. 2010, ApJ, 722, 566